REVIEW

Check for updates

Graphene oxide touches blood: *in vivo* interactions of bio-coronated 2D materials

V. Palmieri, [ID] *[ab] G. Perini, [ID] [a] M. De Spirito [ID] [a] and M. Papi [ID] [a]

Graphene oxide is the hot topic in biomedical and pharmaceutical research of the current decade. However, its complex interactions with human blood components complicate the transition from the promising *in vitro* results to clinical settings. Even though graphene oxide is made with the same atoms as our organs, tissues and cells, its bi-dimensional nature causes unique interactions with blood proteins and biological membranes and can lead to severe effects like thrombogenicity and immune cell activation. In this review, we will describe the journey of graphene oxide after injection into the bloodstream, from the initial interactions with plasma proteins to the formation of the "biomolecular corona", and biodistribution. We will consider the link between the chemical properties of graphene oxide (and its functionalized/reduced derivatives), protein binding and *in vivo* response. We will also summarize data on biodistribution and toxicity in view of the current knowledge of the influence of the biomolecular corona on these processes. Our aim is to shed light on the unsolved problems regarding the graphene oxide corona to build the groundwork for the future development of drug delivery technology.

1. Introduction

Recent years have seen the explosion of biomedical research on graphene-based materials (GBM), owing to the captivating physical and chemical properties of this family of nano-materials.[1] Thousands of scientific papers have been published since 2010, the year Geim and Novoselov received the Nobel Prize for research on graphene; it was pointed out recently that as the number of works continues to grow, "the graphene community could be easily overwhelmed by the collection of this vast knowledge".[2] The nomenclature given to GBM as well as the various methods of synthesis represent a source of confusion since in some papers, what authors describe as graphene/functionalized graphene is another member of this ultrathin carbon family.[3] This leads to (sometimes apparent) contradictions in the results ascribed to the same GBM.

In this review, we will shed light on these inconsistencies and sum up the current knowledge about the *in vivo* bio-interface of freely suspended monolayers of graphene oxide (GO). We focus on GO since the low-cost production and hydrophilic nature of this material still make it preferable to other carbon materials.[4] The effects of GO on biological systems are often compared to its reduced form, reduced graphene oxide (rGO). Like GO, rGO can be obtained with

several protocols and can be characterized by variable C/O atom ratios. In some works, GO has been compared to GBMs that are different from rGO. In this review, we will stick to the nomenclature used in the original papers, and we will also describe the size data available to facilitate the readers in making comparisons.

The *in vivo* fate of nanomaterials is generally influenced by several factors, including the route of administration, nano-material chemistry and physiological environment.[5] Numerous physicochemical characteristics including lateral size, shape, dose, exposure time, number of layers, chemical composition, surface charge, stability, purity, and surface functionality can influence the fate after injection, when materials are exposed to the rich milieu of blood proteins.[6] The proteins in the bloodstream cause an immediate and dramatic change in the biological "identity" of nanomaterials. The result is the develop-ment of a new interface, consisting of a dynamic shell of blood macromolecules. This layer, given the protein enrichment, is usually referred to as the protein corona or the biomolecular corona (BC).[7] The BC determines the interactions with cells, uptake and clearance and therefore affects the biodistribution and delivery to the intended target sites.[8]

The BC of GO is still poorly explored and few works have considered the influence of this layer on *in vitro* and *in vivo* effects. Here, we will first discuss the surface features of GO and their links to amino acids and blood protein binding. Then, we will discuss the GO BC composition and how the BC can influence interactions with blood cells. Finally, we will highlight biodistribution and biosafety concerns as well as

[a] *Fondazione Policlinico A. Gemelli IRCSS-Università Cattolica Sacro Cuore, Largo Francesco Vito 1, 00168, Roma, Italy. E-mail: valentina.palmieri@unicatt.it*
[b] *Istituto dei Sistemi Complessi, Consiglio Nazionale delle Ricerche (ISC-CNR), Via dei Taurini 19, 00185 Roma, Italy*

future challenges related to the development of intravenously injected GO-based pharmaceutical systems. The comprehension of these aspects is involved in and will improve the future design of injectable biocompatible GO.

2. The GO and rGO chemistry

GO and rGO are often defined as bidimensional materials but only pristine graphene (the freely suspended single-atom-thick sheet of hexagonally arranged, sp[2]-bonded carbon atoms[3]) can be considered a true 2D material.[9] GO is a chemically modified graphene derived from the oxidation and exfoliation of graphite and rGO is produced from GO with several possible reduction protocols in order to obtain the closest material to pristine graphene.[3] rGO can be obtained by methods like thermal reduction at high temperature ($>900\ ^\circ$C),[4] chemical reduction by reducing agents (like borohydrides, aluminum hydride, hydrohalic acid and sulphur-containing reducing agents),[2]

hydrothermal, electrochemical and bacteria-mediated reduction.[10] Since residual functional groups and defects remain on the basal plane, rGO is not analogous to pristine graphene.

GO is primarily composed of carbon, oxygen and hydrogen atoms with a C/O ratio between $\sim$1.5 and 2.5. Several possible GO structures have been proposed.[2] Based on the widely accepted Lerf–Klinowski model (see Fig. 1a adapted from ref. 11), the GO basal-plane is highly populated with hydroxyls and epoxides while the edges mainly consist of carboxyl and carbonyl groups. Further, two regions in the GO plane can be distinguished: one region made up of lightly functionalized carbons, predominantly sp[2]-hybridized carbon (graphene-like) atoms, and a second region of highly oxygenated, predominantly sp[3]-hybridized carbon atoms.[12] Due to the distribution of functional groups, the edges of GO sheets are hydrophilic, whereas the basal plane is mostly hydrophobic, and the result is a giant amphiphilic sheet-like molecule.[12] Interestingly, thermal annealing procedures at 80 $^\circ$C for 1–9 days can modify the distribution of the surface groups. During annealing,
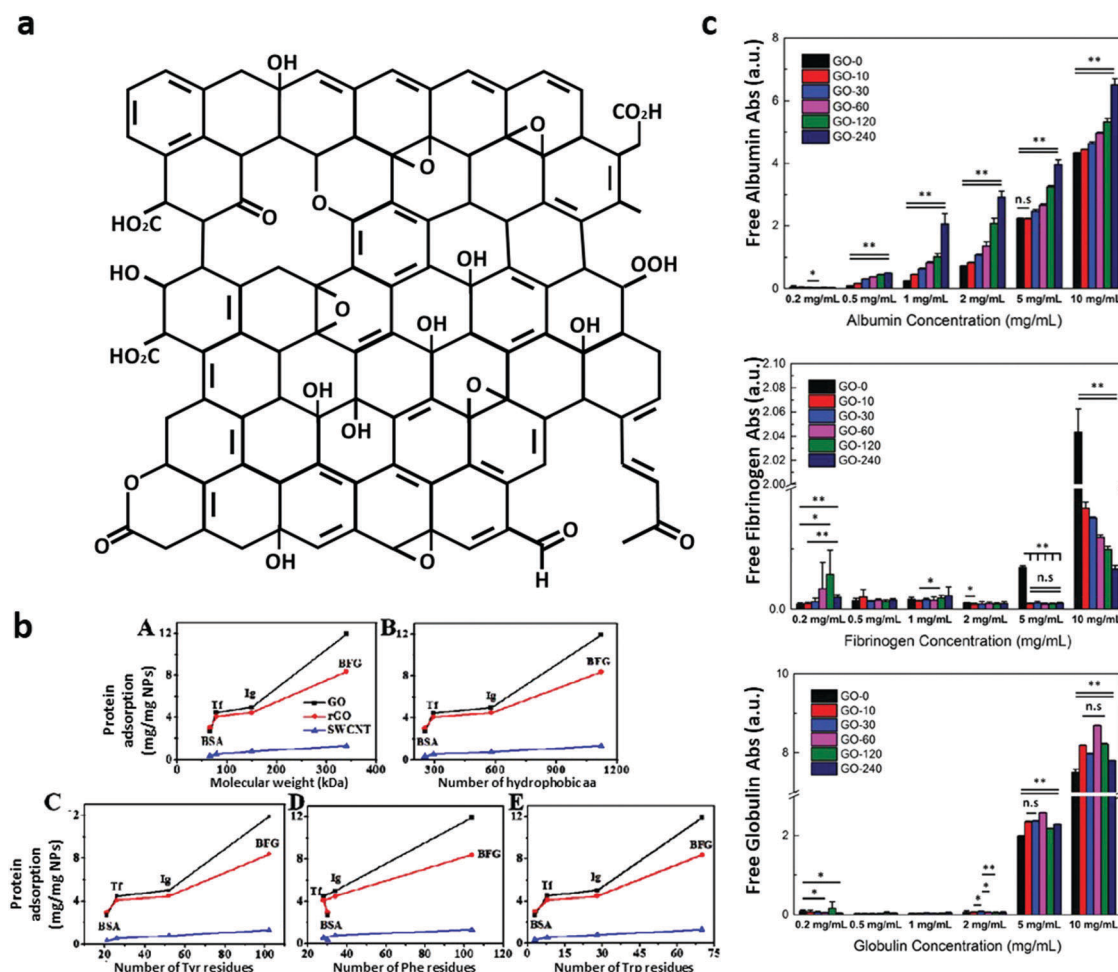
Fig. 1 (a) The Lerf–Klinowski model of the GO structure, adapted[11] with permission from The Royal Society of Chemistry. (b) Analysis of protein residue content and the correlation with the protein adsorption capacity on GO, rGO and single-walled carbon nanotubes (SWCNT). (b) The positive correlations between the protein adsorption capacity and protein molecular weight (A), the number of hydrophobic amino acids (B) and the number of Tyr (C), Phe (D), and Trp (E) residues, adapted with permission from ref. 25, American Chemical Society, Copyright (2015). (c) The binding of albumin, fibrinogen and globulin depends on the lateral size and concentration of GO, as shown in this figure adapted[6] with permission from The Royal Society of Chemistry.

clusters of oxygen functionalities are created on the GO surface without reduction to rGO ($\sim$30% of oxygen content).[13]

GO abundant surface oxygen groups provide plenty of reaction sites for linking external species like proteins, enzymes, peptides, bacteria, cells, and nucleic acids.[12,14]

GO conversion to rGO produces variations in the physical and surface properties and consequently alters the stability in solution and interactions with biological systems.[11,15,16] rGO is indeed more unstable and hydrophobic and tends to form aggregates in solution.[17] Given the variety of reduction approaches and, consequently, the possible surface features produced, it is not surprising that contrasting results have been reported on the biological systems.[4,18,19]

The groups on the GO surface provide unique opportunities for chemical modification via covalent bonds to obtain functionalized GO. The functionalization of GO can be divided into two categories: edge functionalization (of carboxyl groups) and basal plane functionalization (of hydroxyl and epoxide groups). Reactive intermediate functionalization of rGO to directly functionalize the sp^2-hybridized basal plane is also possible; further details can be found in other reviews.[11] Often, GO functionalization is used to build GO-based polymer composites to enhance the thermal and mechanical stability of the original polymer. These composites can be produced by covalent modification of GO functional groups or via non-covalent interactions, taking advantage of hydrogen bonding and van der Waals forces between the polymer and GO.[11,20] Also, the protein adsorption on GO and rGO can occur via covalent or non-covalent interactions. Covalent binding is based on chemical reactions between the side groups of amino acids and functional groups available on the GO surface.

In blood, non-covalent adsorption occurs through weak van der Waals forces, hydrophobic, electrostatic, and π–π stacking interactions.[12,21] The sp^2 hybridized honeycomb carbon lattice of rGO and GO is hydrophobic and, therefore, interacts with the hydrophobic regions of proteins, according to the protein geometry.[9,22] The basal plane of the GO is also enriched with π electrons, making π–π stacking interactions possible. At the same time the oxygen groups of GO, whose composition is strictly dependent on preparation and storing conditions,[2] allow further hydrogen bonds and electrostatic bonds.[12] These electrostatic bonds are strongly influenced by the charge on the proteins and therefore by the pH and the ionic strength of the buffer. Bonding on GO can also be mediated by van der Waals interactions.[23] However, while the electrostatic interactions are more pronounced on GO, both van der Waals and electrostatic interactions play a major role in the adsorption of proteins on rGO due to the increase in the non-functionalized area on the surface.[24] In the following sections, we will show how functionalization of the GO surface alters protein adsorption and consequently BC properties.

3. Blood protein interactions with GO and rGO

Several methods have been used to study the interactions between GO/rGO and proteins. Intrinsic protein fluorescence or light adsorption can be used to monitor the amount of protein bound to nanomaterials.[25] Alternatively, the bicinchoninic acid assay can be used to quantify the total unbound protein quantities.[26] When using these methods, one should bear in mind that the centrifugation step should be adapted to the size of GO flakes used, to allow separation from unbound proteins. As an example, a centrifugation speed of 10 000 rpm can isolate flakes having an average lateral size of 120 nm, while ultracentrifugation at 30 000 rpm is necessary for an average flake's lateral size of 75 nm.[27]

Fluorescence quenching spectroscopy is a convenient technique for investigating protein binding since GO is known to be a universal quencher of fluorescent dyes and aromatic residues (tryptophan (Trp), tyrosine (Tyr)), peptides and proteins, due to strong π–π interactions with the molecules.[6,28,29] From the fluorescence quenching data, the quenching efficiency, association and dissociation constants, and binding cooperativity can be estimated.[6,30] The quenching mechanism of GO has been recently investigated with a technique based on a tunable silica spacer to adjust the distance between GO and fluorophores.[31] It was demonstrated that the quenching mechanism of GO depends on the distance from the fluorescent molecule. The exchange of electrons occurs at very short donor–acceptor distances (Dexter transfer), while when the distance is increased, the main mechanism of quenching is the Förster transfer (FRET), which is efficient even at distances greater than 10 nm in the case of GO as the acceptor.[31] The quenching of blood proteins has selective concentration-dependent effects.[32] Although the fluorescence of blood plasma proteins depends on three aromatic residues, i.e., tryptophan (Trp), tyrosine (Tyr), and phenylalanine (Phe), Trp represents the dominant source of absorption and intrinsic emission. The Trp fluorescence is strongly influenced and highly sensitive to its local microenvironment; fluorescence is high when Trp is in the hydrophobic core of the protein, and weak when it is exposed to a hydrophilic solvent. Generally, GO quenches Trp of the three plasma proteins, namely, albumin, globulin, and fibrinogen. However, it displays a selective amplification of fibrinogen fluorescence at concentrations below 3 μg mL^{-1}. As explained in the study by Kenry and colleagues, the small sizes of albumin and globulin allow efficient quenching due to the physical wrapping by the GO nanosheets and energy transfer between GO and plasma proteins caused by the π–π stacking and interaction.[32] Conversely, the large fibrinogen size does not allow GO wrapping at low concentrations. This causes a slight increase in the intrinsic fluorescence of fibrinogen, thanks to the GO-induced aggregation of this protein. This study highlights how, for GO and GBM nanomaterials, a careful choice of methods and evaluation of concentration-dependent effects should be made by researchers.[33]

Protein binding constants on GO can be obtained by the surface plasmon resonance technique[25] and the mechanism of binding can be derived by isothermal titration calorimetry and by performing quenching experiments at varying pH values (to study the influence of electrostatic interactions).[30] After labeling with convenient probes, the protein interaction with

Table 1 Amino acids and blood protein adsorption on GO

	Material	Main conclusions	Ref.
Amino acids	Few-layer graphene (FLG), ~5–6 layers, (chemical exfoliation of graphite) GO (Hummers' method) ~6–8 nm thickness, avg. area ~25 μm^2	Strong binding of aromatic residues: GO > FLG adsorption of Trp and Tyr, possibly through hydrogen bonds. Phe shows similar adsorption on FLG and GO	35
	GO (lateral dimension 0.5–3 μm, thickness 0.8 nm) rGO (lateral dimension 0.5–3 μm, 1–10 layers) purchased from Chengdu Organic Chemical Company, Chinese Academy of Science	Positive correlations between adsorption capacity and protein molecular weight, hydrophobic and Trp, Tyr, Phe residue content	25
Blood proteins	GO (Hummers' method) with variable lateral size from ~100 nm (small GO) up to ~1000 nm (large GO), thickness 1.3 nm	Albumin is better adsorbed by large GO. γ-Globulin is completely adsorbed up to 5 mg mL^{-1}, and at higher concentrations is better adsorbed by large GO. Fibrinogen is completely adsorbed up to 10 mg mL^{-1} and at higher concentrations is better adsorbed on small GO	6
	GO and rGO see above	Adsorption order: fibrinogen > immunoglobulin > transferring > albumin	25
	GO solution from Sigma-Aldrich (~2 μm and thickness 1 nm) rGO obtained with hydrazine monohydrate reduction protocol (aggregated)	Adsorption order: complement factor H > IgG > albumin Albumin better adsorbed on GO, probably larger surface area available	26
	2D graphene nanoplatelets (GNP) purchased from Cheap Tubes, Inc., Cambridgeport, VT, USA, thickness 10 nm, size of several μm (from atomic force microscopy (AFM) images)	Albumin better adsorbed on GNP	40
	Porous GO (PGO) prepared by the sequential acid and base treatments of GO synthesized through the Hummers' method (Fig. 2e), thickness 2–4 nm, size of several μm (from AFM images)	Fibrinogen and γ-globulin better adsorbed on PGO	

GO can be analyzed by using fluorescence correlation spectroscopy and fluorescence lifetime imaging microscopy.[34] Protein conformational changes can be analyzed via circular dichroism and also by the red shifting of the fluorescence peak that occurs with Trp residues when exposed to a more hydrophilic environment.[30]

Experimental data on GO interaction with amino acids and proteins are given in Table 1, where the physiochemical features of GO or GBM reported in each paper are also summarized. When GO and graphene, having a thickness of 5–6 layers (hence a few-layer graphene (FLG) according to literature[3]), were incubated with amino acids, both interacted strongly with Trp, Tyr, and Phe. GO showed significantly higher adsorption for Trp and Tyr, possibly through hydrogen bonds, compared to FLG, which exhibited π–π interactions. Phe showed similar adsorption on FLG and GO.[35] Also, molecular dynamics (MD) studies indicated that GO nanoflakes and amino acid complexes are stabilized by hydrogen bonding interactions, whereas graphene nanoflake complexes are stabilized by π–π interactions, leading to enhanced binding energies for GO nanoflake complexes.[36]

As shown in Fig. 1b, Chong et al. demonstrated positive correlations between the adsorption capacity of GO, rGO and single-wall carbon nanotubes (SWCNT), and protein molecular weight, hydrophobic residues and Trp, Tyr, Phe residue content.[25] The data indicate that surface atoms, as well as buried residues, are involved in the phenomenon once the protein partially unfolds and adsorbs on the carbonaceous surface.[25] Basic residues, such as arginine, were observed to play an equally crucial role in the adsorption of blood proteins.[37,38]

Experiments on the interaction between GO and purified blood proteins have been focused on the most abundant components in human plasma: albumin, fibrinogen and γ-globulin.[6] As shown in Fig. 1c, GO samples with variable lateral sizes (LS) have been used to study the influence of the amount of available surface on protein adsorption and the behavior of these proteins on GO was largely different.[6] In this work, albumin, fibrinogen and γ-globulin proteins were incubated with 'small GO sheets', having LS of ~100 nm, obtained after 240 minutes of sonication, to progressively larger sheets up to ~1000 nm LS of unsonicated 'large GO sheets'. Albumin, a small transport protein and the most abundant protein in human plasma, has maximal adsorption on large GO sheets and its secondary structure is minimally perturbed following the adsorption.[6] Nevertheless, the functionality of albumin is reduced when it is adsorbed to GO.[30] Indeed, epoxy groups on GO crosslink with the surface of albumin, probably masking binding sites and impeding bilirubin binding.[30] in contrast, in GO-COOH, obtained through the oxidization of epoxy and hydroxyl groups on the GO surface to carboxyl groups by chemical modification with sodium chloroacetate, the addition of carboxyl groups to the GO surface masks epoxy groups and consequently the albumin functionality is preserved.[39] γ-Globulin, the second most abundant plasma protein, remains stable after interaction with GO but is poorly affected by the size of GO sheets to which it interacts in the range between ~100 nm and ~1000 nm. Only at high concentration is γ-globulin better adsorbed by larger GO sheets (~1000 nm), while at concentrations up to 5 mg mL^{-1} globulin saturates binding sites and is not visible in the supernatant.[6] Fibrinogen, a large protein of the coagulation system, is denatured on GO and is better adsorbed on smaller GO sheets.[6]

Chong and colleagues reported that for both GO and rGO, the order of adsorption is fibrinogen > immunoglobulin > transferrin (the iron-binding blood plasma glycoproteins that control the free iron level in biological fluids) > albumin.[25]
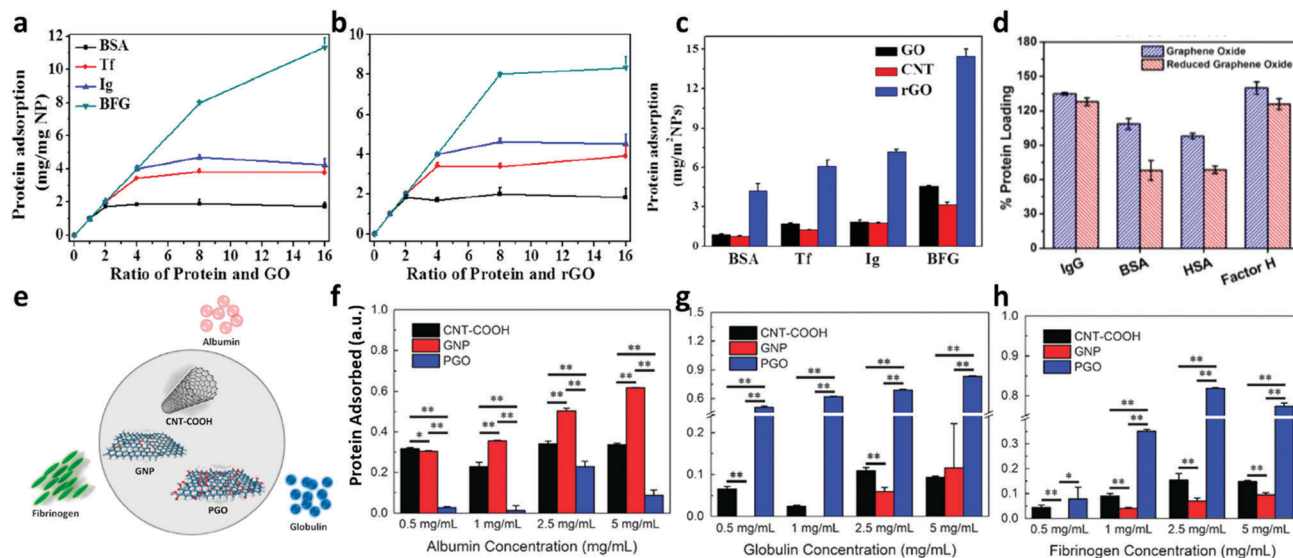
Fig. 2 Milligrams of proteins (bovine serum albumin (BSA), transferrin (Tf), immunoglobulin (Ig) and bovine fibrinogen (BFG)) adsorbed on GO (a) and rGO (b); adapted with permission from the American Chemical Society, Copyright (2015).[25] Data for adsorption corrected for available surface indicate a higher capacity of rGO in respect to other materials (c). Comparison between GO and rGO loading of immunoglobulin g (IgG), BSA, human serum albumin (HSA) and factor H; reproduced with permission from ref. 26. (d) Protein adsorbed on three materials, namely carboxylic-functionalized multi-walled CNT (CNT-COOH), 2D graphene nanoplatelets (GNPs) and porous graphene oxide (PGO) illustrated in (e), are reported in (f) albumin, (g) globulin and (h) fibrinogen; adapted with permission from ref. 40.

Similar to Chong, in the study of Belling on GO and rGO, the order of protein adsorption is as follows: complement factor H > IgG > albumin.[26] These data are in agreement with the Kenry study, since albumin appeared in the supernatant even at very low concentrations (0.5 mg mL^{-1}) followed by globulin and fibrinogen, and was visible in the supernatants at 5 and 10 mg mL^{-1}, respectively (Fig. 1b and ref. 6).

The direct comparison of rGO and GO protein binding capacity is difficult because (i) rGO is less stable and its exposed surface varies, and (ii) the rGO synthesis procedure varies among different studies. Chong utilized GO and rGO with lateral dimension between 0.5 and 3 μm from a commercial source, and although adsorption onto rGO was somewhat diminished when juxtaposed with GO (Fig. 2a and b), especially for fibrinogen, the authors concluded that significant differences between these two materials were not visible.[25] Belling, who synthesized rGO by chemical reduction, indicated a higher albumin loading of GO caused by the less available binding surface of partially aggregated rGO.[26] This effect was less visible for IgG and complement factor H; however GO seemed to better adsorb protein in general (Fig. 2d). It should be noted that in both studies, the rGO was unstable and tended to form multilayers or aggregate. Chong considered this effect and normalized the milligrams of protein adsorbed to the available surface, and surprisingly rGO was more efficient in protein loading (Fig. 2c), which is consistent with the idea that π–π and hydrophobic interactions are the primary driving forces during protein binding (Chong, Ge et al., 2015).[25]

To analyze the influence of oxygen functionalities using materials with similar solubility, Kenry and his group selected carboxylic-functionalized multi-wall nanotubes CNT (CNT-COOH), 2D graphene nanoplatelets (GNPs) and porous graphene oxide (PGO)

(Fig. 2e). Results from the work are reported in Fig. 2f (albumin adsorption), Fig. 2g (globulin adsorption) and Fig. 2h (fibrinogen adsorption). The highest loading capacity for albumin was displayed by GNP, followed by CNT-COOH and PGO, suggesting that the associations might be strongly dependent on the hydrophobic interactions via π–π stacking between the aromatic rings of hydrophobic amino acids and the carbon nanomaterial surface. A reverse trend was observed for globulin and fibrinogen, where PGO displayed the highest capacity loading for both proteins, while those of CNT-COOH and GNP were similar. The lower adsorption of fibrinogen on CNT-COOH and GNP confirms Chong data and might be due to the larger size of fibrinogen.[25] As such, fibrinogen adsorption might require a higher surface area. However, globulin is also poorly adsorbed on CNT-COOH and GNP, so the authors ascribed the difference in adsorption to the amount of oxygen functional groups on the surface.[40]

In summary, the adsorption capacity of GO is influenced by the aromatic residue content, protein size and hydrophobicity. Fibrinogen is better adsorbed than albumin by GO, while GNP, which is less oxygenated, better adsorbs albumin. The hydrophobic interactions between protein amino acids and poorly oxygenated GBM are less-favoured due to the instability of these nanomaterials. Further systematic studies are needed to clarify the influence of surface groups and nanomaterial dispersibility on protein adsorption.

4. The composition of the GO biomolecular corona

In the journey of GO after injection in our body, the first process that occurs is undoubtedly the binding of plasma
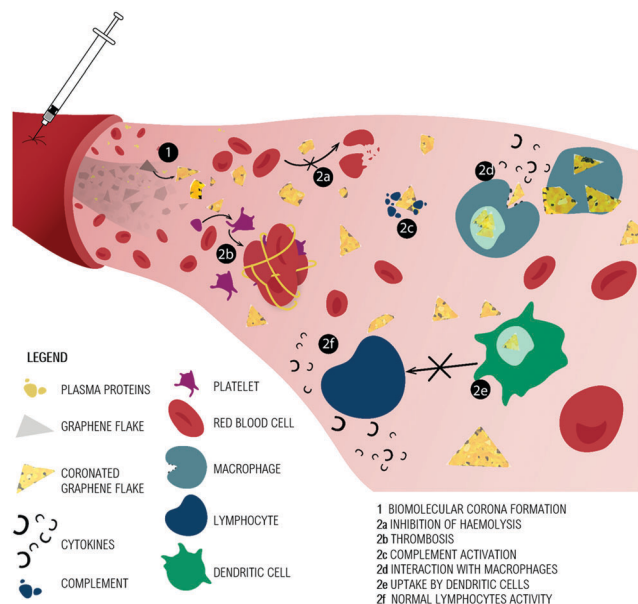
Fig. 3 Main results of GO interaction with blood components are summarized in this illustration of the injection of GO flakes in the bloodstream. The formation of the BC (1) prevents the hemolysis of red blood cells (2a). Thrombosis (2b) and interaction with complement proteins (2c) are ascribed to GO. In (2d) some of the possible fates after macrophage encounters are shown: extracellular blocking or intracellular uptake. The release of cytokines occurs when macrophages uptake GO. Aggregates of GO in macrophage cytoplasm induce the production of pro-inflammatory cytokines. Dendritic cells fail to present antigens to lymphocytes when they uptake GO (2e). Lymphocyte activity is not inhibited, and BC protects lymphocytes from apoptosis (2f).

proteins on its surface (see Fig. 3-1). Intravenously injected nanoparticles encounter multiple lines of defense intended to neutralize the invaders. The first and most critical defense line is the blood protein adsorption and formation of the

biomolecular corona (BC).[41] Of the thousands of proteins present in our body, 10 to 50 may take part in a nanomaterial BC.[42] The subset of blood proteins that have been identified in at least one nanomaterial BC has been named "adsorbome".[43] Adsorbome is made of a total of 125 proteins divided into highly and poorly abundant components by a threshold of 10% of the total protein mass.[43] The BC appears to follow a general structure: up to six proteins are adsorbed at high abundance, and many more are adsorbed in low quantity. BC is species-specific and there are only a few proteins in common among human and mouse BC.[42]

Studies on the BC composition of GO and GBM are limited (Table 2). We will first consider the major issue in the characterization of the BC of these nanomaterials: their instability in solution, which differs from ultrapure water. rGO, pristine graphene and, to a lesser extent, GO are prone to aggregation in saline solution, phosphate buffered saline (PBS) and of course plasma and serum.[17,33,44] To overcome this problem, the BC of pristine graphene (G-BC) has been analyzed on solid substrates in polystyrene wells or after direct exfoliation of graphite in human serum. On graphene substrates (G-substrates), obtained by chemical vapour deposition, the authors tested human plasma concentrations from 2% up to 70%[45] and found that plasma concentration influenced BC composition. Albumin was the only attached protein on G-substrates at plasma concentrations below 5%. With increasing concentrations of plasma, first prothrombin and alpha-fetoprotein were added to the BC, and then vitamin D binding protein and fibrinogen beta chain enriched the BC. At the highest plasma concentration the proteins adsorbed were inter-alpha-trypsin inhibitor heavy chain, thrombospondin-1, complement component C7, prothrombin, serum albumin, alpha-fetoprotein, fibrinogen alpha chain, C4b-binding protein alpha chain, kininogen-1, vitamin D-binding protein, fibrinogen beta chain, and cyto-

Table 2 Pristine graphene and GO BC in human plasma/serum

	Material	Main components of the biomolecular corona	Ref.
Pristine graphene	Pristine graphene substrates on polystyrene obtained by chemical vapor deposition	Inter-alpha-trypsin inhibitor heavy chain, thrombospondin-1, complement component C7, prothrombin, serum albumin, alpha-fetoprotein, fibrinogen alpha chain, C4b-binding protein alpha chain, kininogen-1, vitamin D-binding protein, fibrinogen beta chain, and cytochrome (70% plasma concentration)	45
	Graphene (direct exfoliation of graphite in serum), lateral size 200–300 nm, thickness 25 nm (protein layer attached)	Albumin, lipoproteins (mainly apolipoprotein A-1 and apolipoprotein E), and vitronectin	46
Graphene oxide	GO purchased from Graphene Supermarket (USA), flake size 0.5–5 µm, thickness 1.1 nm	Transport, immune response protein, complement factors, apolipoprotein E, inter-alpha-trypsin inhibitor heavy chain H1, H2 and hyaluronan-binding protein 2 (in serum)	49
	GO purchased from Nanjing XFNANO Materials Tech. Co., Ltd, Nanjing, China lateral size 0.5–5 µm and thickness of 0.7 nm	95% consists of organic molecules, ornithine, octadecenoic acid, dodecanol, talose, and tetradecanoic acid show selective accumulation (14 days in plasma)	54
	GO (lateral size few µm) and nGO-PEG (10–50 nm)	nGO-PEG has reduced protein binding and selectivity toward six proteins: four immune-related factors (C3a/C3a (des-Arg), clusterin, histidine-rich glycoprotein, vitronectin) in serum	55
	GO, GO-NH$_2$, GO-PAM, GO-PAA and GO-PEG	Protein adsorption GO > GO-PAM > GO-NH$_2$ > GO-PAA > GO-PEG	56
	Size of 100–500 nm, thickness depends on functionalization (PAM, PAA or PEG became higher than GO with 2.9, 2.6 and 4.1 nm thickness, vs. 1.1 nm, respectively)	IgG highly adsorbed GO > GO-NH$_2$ > GO-PAM > GO-PAA > GO-PEG. Influenced by surface modification include thrombospondin 1, gelsolin and hemoglobin (less abundant in GO) in serum	

chrome.[45] Interestingly, most of these proteins are not part of the "high abundance" adsorbome defined by Walkey and Chan.[43]

Direct exfoliation of graphite in human serum is a recently established ultra-sonication protocol to analyze the BC of pristine graphene.[46] This method was developed by Castagnola and colleagues to avoid the usage of dispersants that form an adsorbed layer on the graphene surface and affect BC composition. The method consists of 1 to 4 hours of ultrasonication of 10 w/v% of natural flake graphite dispersed in a solution of serum at different concentrations using a bath sonicator.

In this paper, the authors found that G-BC is composed of albumin, lipoproteins (mainly apolipoprotein A-1 (ApoA-1) and apolipoprotein E (ApoE)), and vitronectin.[46] The serum concentration seems to slightly affect the G-BC composition in this work. The available epitopes exposed include abundant ApoA-I, which is known to be involved in early biological interactions, both at the cell and organ level.[46,47] Despite the different available surfaces and other physiochemical properties that are known to vary between graphene in solid or soluble form, the markedly different compositions of the corona might arise from the protein source used in the experiments, *i.e.* plasma and serum.[45,46] Indeed, while incubation of nanomaterials in serum is known to create a BC mainly formed by apolipoproteins, in plasma, coagulation and complement factors may also participate.[48]

In a direct comparison of serum BC of GO and other carbon-based nanomaterials, *i.e.*, carbon black (CB) and multi-walled carbon nanotubes (MWCNT), GO has the lowest affinity for albumin because of its lower hydrophobicity, and a higher adsorption capacity for low-abundant proteins of serum.[49] These data agree with the single protein studies of Kenry, discussed in the previous section.[6,40] In another work, BC formed in foetal bovine serum (FBS) shows that the adsorption of protein is reduced when surface groups are reduced (rGO), and that high material concentration also induces lower adsorption efficacy.[50] With respect to CB or MWCNT, greater amounts of proteins, especially complement components and blood coagulation proteins, are adsorbed on GO corona. The authors explained this higher protein concentration with the low surface curvature of GO, combined with negatively charged functional groups and high surface area availability. These features result in several possible interactions, *i.e.*, hydrogen bonding and electrostatic interactions, in addition to hydrophobic and van der Waals interactions of other nanomaterials.[49,51] The proteins identified in GO-BC are mainly involved in transport and immune response.[49] All investigated nanomaterials possessed a BC enriched with complement factors and apolipoproteins (involved in targeting and translocation through the blood–brain barrier) but apolipoprotein-E is selectively adsorbed by GO. A particularly high number of complement factors was found in GO-BC, together with proteins involved in hemostasis and tissue structuring (hyaluronan-binding proteins, namely inter-alpha-trypsin inhibitor heavy chain H1, H2 and hyaluronan-binding protein 2).[49] Qualitative protein analysis shows that BC of GO is influenced by the health conditions of blood donors, as demonstrated for other nanoparticles.[52,53] Indeed, GO sheets incubated with plasma from patients with different diseases/conditions, including hypofibrinogenemia, blood cancer, thalassemia major, thalassemia minor, rheumatism, fauvism, hypercholesterolemia, diabetes, and pregnancy, and analysis by gel electrophoresis showed significant variations in the compositions of the BC. These differences can be attributed to alterations in the plasma protein compositions/content, the protein conformation, and/or the protein solubility.[52]

When GO is submerged in human plasma for the long-term (14 days) a biotransformation and reduction to rGO occurs, mediated by free radicals.[54] During this period, the BC formed is principally made by small organic molecules that account for 95% of the corona composition. Some molecules, such as ornithine, octadecenoic acid, dodecanol, talose, and tetradecanoic acid show a selective accumulation on GO.[54]

Surface modification is a commonly adopted approach to improve the biocompatibility of GO and to control the formation of the BC.

Tan and colleagues compared the interactions of serum proteins with GO and nGO-PEG, a nanometric GO functionalized by a 10 kDa amine-terminated six-arm-branched polyethylene glycol (PEG) *via* amide formation.[55] Unlike GO, which adsorbs a significant amount of serum proteins without specificity, nGO-PEG exhibits reduced protein binding and selectivity toward six proteins: four immune-related factors (C3a/C3a (des-Arg), clusterin, histidine-rich glycoprotein, vitronectin) and two coagulation factors (contained platelet factor 4 and thrombin). However, the association of thrombin and platelet factor 4 might be a pseudo effect, since their circulation levels are extremely low, but increase by more than 3 orders of magnitude during the clotting protocol in serum preparation.[55] Further, given the size difference between nGO-PEG (nanometric flakes) and GO (micrometric flakes), the potential size effect on the above interactions should be investigated.

Xu and colleagues measured the effect of GO surface modification on the composition of GO-BC in mouse serum (Fig. 4). GO was chemically modified to obtain aminated GO (GO-NH$_2$), prepared with GO dispersion in ammonia with hydrazine hydrate as a reducing agent, GO-polyacrylamide (GO-PAM), GO-polyacrylic acid (GO-PAA) and GO-PEG.

GO (100%) and GO-PAM (90.2%) showed higher protein adsorption with respect to GO-NH$_2$ (54.3%), GO-PAA (39.3%) and GO-PEG (43.9%), presumably due to their different surface charges and hydrophobicities. The relative amount of IgG in the BC was much greater than other proteins, and a big difference was observed among GO (62.2%), GO-NH$_2$ (58.3%), GO-PAM (52.3%), GO-PAA (36.8%) and GO-PEG (30.2%).[56] Other proteins influenced by surface modification include thrombospondin 1, gelsolin and haemoglobin (less abundant in GO).[56]

Another functionalization strategy to modify GO-BC foresees the spontaneous self-assembly of chitosan (CS) and GO *via* electrostatic interactions to form CS-GO, which has a reduced BSA and lysozyme adsorption capacity, and, in FBS, a reduction of serum proteins uptake.[57]

In summary, the composition of G-BC is affected both by the nanomaterial state and the protein source. We can speculate that
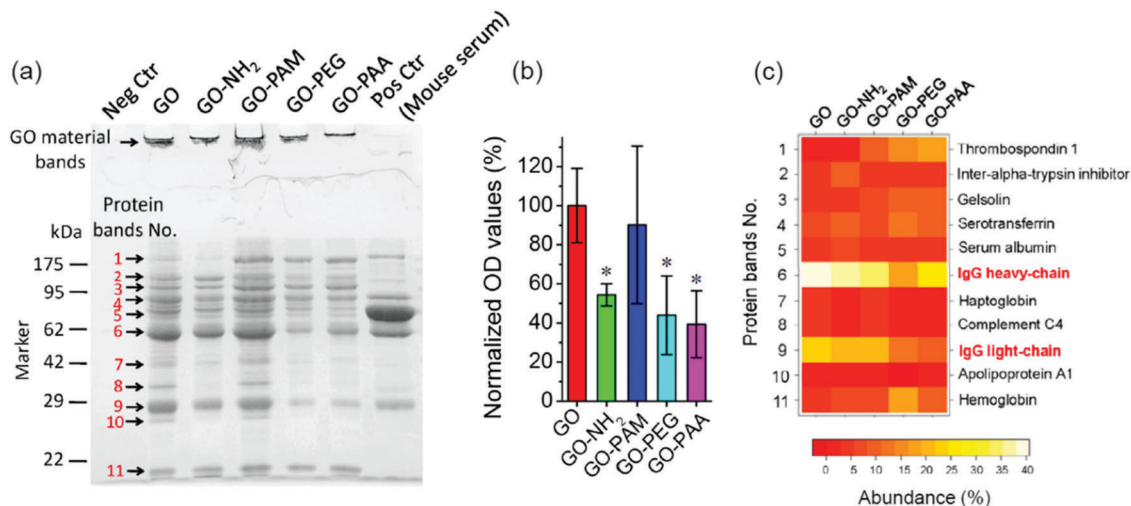
Fig. 4 Protein corona analysis of GO, GO-NH2, GO-PAM, GO-PAA and GO-PEG formed in mouse serum at 37 °C for 1 h. (a) SDS-PAGE analysis of protein corona. (b) Normalized OD values of each protein corona, indicating the amount of protein adsorbed on GO. Asterisks (*) denote $p < 0.05$ compared to pristine GO. (c) Eleven highly abundant components identified by mass spectrometry. Reproduced with permission from ref. 56.

the work of Castagnola and colleagues[46] defines, to some extent, the configuration of the BC of injected pristine graphene and that the enrichment in apolipoproteins might be useful for targeted delivery applications (as discussed in the conclusions). However, unfunctionalized pristine graphene instability remains the Achilles' heel of this nanomaterial. As we will see in Section 6, when GO is injected in blood, aggregates form, but in a size and dose-dependent fashion.[58] This means that GO is more stable and is suitable for an injected delivery system and consequently, its BC should be precisely controlled. GO adsorbs a large amount of proteins thanks to the highly available surface,[49] and this is generally looked at as a disadvantageous feature *in vivo*, since the more proteins "mark" the foreign nanomaterial, the better it is attacked by our immune system.[59] Many functionalization strategies are therefore exploited to improve GO stealth properties. However, this protein enrichment gives GO some advantages over other nanomaterials in diagnostics and pharmaceutical applications. Indeed, the higher protein adsorption in the BC can be exploited to select and enrich poorly concentrated biomarkers in patients' blood[52] and develop diagnostic tools based on the BC.[7] Secondly, the list of proteins found in GO-BC includes ApoE, vitronectin and clusterin, which are important blood–brain barrier (BBB)-directing molecules (ApoE) as well as targets of therapies (Table 2).[60–62] rGO, whose BC, to the best of our knowledge, still has to be fully characterized, can enter the brain thanks to a transitory decrease in the BBB paracellular tightness.[63] Future studies could be focused on delivery applications based on GO/rGO selectively adsorbed proteins.

5. Effects of bio-coronated GO materials on blood components

BC composition directly influences interactions with other blood components (Fig. 3-2). For example, the presence of

antibodies, complement and clotting factors in the nanoparticle BC may activate clotting and coagulation cascades. Further, the BC coating can promote phagocytosis and elimination from the circulation.[41]

We will first consider data on the GO interaction with the red blood cells (RBCs), given in Table 3. An intravenously injected nanomaterial is likely to interact first with RBCs rather than other cells, due to their abundance in blood. Hemolysis represents the damage to RBCs that leads to the leakage of hemoglobin into the bloodstream. After hemolysis, the nanomaterial may adsorb released hemoglobin and/or adhere to cell debris, which can increase its likelihood of elimination by macrophages.[8] Although the literature is contradictory regarding GO effects on RBC, when BC is introduced into the framework the results become clearer. Due to the sharp edges of GO and rGO, hemolytic effects might be expected *in vivo*, possibly caused by nanomaterial blades disrupting cell membranes, as reported for GO interactions with bacteria.[19]

Feng and colleagues discovered RBC morphological alterations and aggregation above 100 μg mL^{-1} and hemolytic effects above 10 μg mL^{-1} reaching 96% at 500 μg mL^{-1}.[64] Lower hemolytic concentrations have been reported by other groups.[65] Small GO flakes (few hundreds of nm) seem to be more destructive.[66–68] The aggregation and hemolysis might be driven by the hydrophobic interaction between the GO surface and the lipid bilayer of RBCs, or other nonspecific interactions such as hydrogen bonding between the glycocalyx and hydroxyls and carboxyls of GO could also take place.[64] Alternatively, binding between charged groups on the GO surface and positively charged phosphatidylcholine of the RBC membrane could explain this interaction, but aminated rGO (G-NH$_2$) does not induce hemolysis.[65,66] Even the stability in solution is known to play a role in the GO interaction with living systems.[33] rGO and pristine graphene, with lower oxygen content, also have lower hemolytic activity but are also more prone to aggregate, yielding fewer cell contacts.[66,68]

Table 3 Haemolytic effects of GO

Material	Hemolysis	BC effects	Ref.
GO (Chengdu Organic Chemistry Co., Chinese Academy of Science) average hydrodynamic diameter $\sim$500 nm	Starts from 10 µg mL^{-1} and reaches 96% at 500 µg mL^{-1}	—	64
GO (graphite oxidation) and G-NH$_2$ (thermal annealing and amination) few layers and 2 µm size	Starts from 2 µg mL^{-1} and reaches 60% at 10 µg mL^{-1} G-NH$_2$ not hemolytic	—	65
GO (Hummers' methods) with size between 300 and 800 nm and rGO from dehydration of GO (size of several µm) Size data refer to the hydrodynamic diameter in water	GO = between 60% and 80% ($\propto$ sheet lateral size) at 200 µg mL^{-1} rGO = 15% at 200 µg mL^{-1}	—	66
Pristine graphene and GO thickness of 0.8 nm	Not hemolytic (<10% at 75 µg mL^{-1})	—	68
GO (Graphene A, Cambridge, USA) hydrodynamic radius from 660 nm to 100 nm (sonication) thickness of 0.8 nm	Between 60% and 80% ($\propto$ sheet lateral size) at 200 µg mL^{-1}	Inhibition of hemolysis if GO is surrounded by a protein corona	67

As explained above, *in vivo* injection implies the formation of the BC around GO and rGO (Fig. 3-1) and regardless of the BC composition, several groups have demonstrated the physical hindrance of BC between GO and eukaryotic cells (Fig. 3-2a). The presence of a BC around GO flakes can completely inhibit the interaction and therefore RBC hemolysis.[67] GO hemolysis is also prevented by chitosan, dextran and curcumin coating or by functionalization of the GO surface.[66,69,70] An interesting study proposed the use of mussel-inspired dopamine (DA) for both the GO reduction and functionalization.[71] DA has many properties: (i) it adheres to solid surfaces in water solution without surface pretreatment; (ii) once on the surface, DA can anchor a secondary functional biopolymer *via* the thiol, imino and amine groups; (iii) the catechol groups of DA can convert GO into chemically reduced rGO. Cheng and colleagues exploited these features to obtain heparin-grafted polyDA-rGO (Hep-gpRGO) and BSA-grafted polyDA-rGO (BSA-*g*-pRGO) that greatly suppressed hemolysis ratios (lower than 1.8%, even with a high concentration of 200 µg mL^{-1}).

These contrasting results are not unique in the literature on GO and cells, but they are explainable by the experimental conditions. In most of the literature, the cytotoxicity of GO and rGO against many cell lines has been demonstrated to be caused by cellular membrane penetration and/or oxidative stress induction.[6,72] However as for RBC, the physical damage to the cell membrane is largely attenuated when GO is incubated with BSA or FBS, due to the extremely high protein adsorption ability of GO.[14,25,39,73,74] In cell culture medium supplemented with FBS, GO is enriched with a BC of albumin and IgG, irrespective of the lateral size GO.[75] In summary, the presence of proteins in the cell culture medium influences the results on cytotoxicity and we could consider that GO and rGO are not hemolytic *in vivo* where abundant protective BC form on their surfaces (Fig. 3-2a).

Hemostasis cascade prevents blood loss from injured tissue and maintains blood fluidity. The final hemostasis is driven by platelets, which form the clot, a mixture of red blood cells, aggregated platelets, fibrin and other cellular elements (Fig. 3-2b). If the clot forms abnormally, it can induce thrombosis.

Thrombogenicity is an important feature evaluated in nanomaterial design for *in vivo* delivery and represents the propensity to induce blood clotting and induce occlusion of a blood vessel by a thrombus.[8]

Nanoparticle thrombogenic properties are largely determined by physicochemical properties and by interaction and modulation of the activity of various components of the coagulation system such as platelets and plasma coagulation factors.[76] Furthermore, nanoparticles engineered to have longer systemic circulation times increase the likelihood of contact with blood components including the coagulation system, with thrombogenicity risks.[8]

In vitro studies on pristine graphene and GO provided evidence that concentrations up to 75 µg mL^{-1}, do not interfere with platelet function or the pathways of plasma coagulation[68] and that GO, up to 50 µg mL^{-1}, does not interfere with platelet aggregation or fibrinogen polymerization.[64] GO completely blocks clotting factors only at high concentrations (*i.e.* $\sim$500 µg mL^{-1}).[64]

Contrasting results have been reported by Singh and colleagues that described few-layer GO sheet (size between 0.2 and 5 µm) induction of platelet activation and thromboembolism *in vivo*. At very low concentrations (2 µg mL^{-1}), GO caused *in vitro* platelet aggregation through the intracellular release of calcium from cytosolic stores, activation of nonreceptor protein tyrosine kinases of the Src family and enhancement of platelet integrin–fibrinogen interactions. When administered *in vivo* (250 µg kg^{-1} body weight), 48% of lung vessels were partially occluded after 15 minutes.[77] Interestingly, the thromboembolisms can be avoided if rGO or GO are covered by a heparin corona.[22,29] This *in vivo* impact on the coagulation cascade can be caused by an aggregation of the nanomaterial after injection.[78] However, rGO is less stable than GO and this hypothesis should be discarded since thromboembolism of rGO is lower, with only 8% of vessels occluded.[77] Another explanation could be that the adsorption of coagulation factors onto the GO corona might cause their contact activation.[76] Changing GO surface groups and creating positively charged amine-modified rGO (N-GH$_2$) at the same concentration (250 µg kg^{-1} body weight) the thrombogenicity is suppressed might influence both the interaction with blood cells and the composition of BC.[56,65]

The group of proteins of the complement system (Fig. 3-2c) that promotes antigen phagocytosis and recruitment of neutrophils and macrophages to the site of inflammation is highly abundant in the GO corona.[49] The *in vitro* GO complement-activation test provided evidence that this material significantly triggers complement activation by the increase in the

concentration of fragments C3a (proportional to GO concentration) and C5a.

Authors have claimed that this activation might be driven by both hydroxyl groups and the hydrophobic surface of the GO skeleton.[64] A detailed study of the relation between GO surface oxidation and complement activation confirmed this hypothesis.[79] In this work, GO was synthesized through the modified Hummers' method and was mildly reduced to obtain three nanomaterials having different oxygen content (i.e. 36%, 29%, 24% atomic percentage) and size of a few μm (from AFM characterization). It was found that the decrease in oxygen content reduced complement activation, as reflected in the lower levels of both C5a and SC5b-9. This could be explained by the instability of the flakes and the diminished exposure of the GO surface in less oxidized GO, which is more prone to forming irreversible flocculates in solution. On the other hand, this phenomenon may be attributed to a combined effect of oxygen-type functionality and topological change arising from a wrinkling of the GO surface that may modulate the affinity for recognized molecules or interaction with complement regulators.[79] Since C5a can substantially potentiate IL-6 production in lipopolysaccharide (LPS)-stimulated peripheral human blood leukocytes, the effect of GO on IL-6 release in human whole blood was tested in the same study. At concentrations below the GO-mediated complement activation, the LPS-induced responses were inhibited by GO, probably through a direct interaction of GO with LPS or GO and LPS binding protein. This effect disappeared when the GO concentration was above the complement activation threshold and the IL-6 cytokine release was induced.[79] Pre-coating of GO or rGO with a corona of albumin or complement H factor, obtained after incubation of the nanomaterials at 37 °C for 2 hours with these proteins, can reduce complement activation by 40% and 90%, respectively.[26] This interesting effect is mediated by both the steric blocking of the interaction with complement components and, for the complement H factor corona, by regulation of the complement cascade.[26] In summary, GO activates the complement system but the reduction of oxygen content and the precoating with BC might prevent this effect.

Complement activation may result in altered biodistribution caused by rapid clearance from the bloodstream via phagocytosis by mononuclear cells. In addition, complement activation can support cell-mediated immunity through the enhancement of B-cell responses and promotion of dendritic cells (DC) and T-cell activation.[8] Understanding the interaction of GO with immune cells is crucial for the development of biomedical technologies and some recent interesting reviews have focused on the mechanisms occurring when GBM interact with immune systems.[18,72,80,81] The results on immune activation are contrasting but we can certainly assume that there is a strict connection between GO size, oxidation and functionalization and effects on immune cells.[18] For example, human peripheral blood mononuclear cells (PBMC), which include lymphocytes, monocytes, and dendritic cells, did not show significant stimulation (proliferation)/immunosuppression (cytotoxicity) below 75 μg mL^{-1} after incubation by either pristine graphene or GO.[68] However, proinflammatory cytokine expression quantification showed that PBMCs treated with pristine graphene expressed relatively higher levels of IL-8 and IL-6 compared to GO samples, thus indicating the inflammatory potential of the former.[68]

A recent study demonstrated that GO induced proinflammatory cytokine expression in a size-dependent fashion, with smaller sized GO (<1 μm) being more effective than larger ones (1–10 μm).[18,82]

Macrophages (Fig. 3-2d), the professional phagocytes of nanomaterials, seem to better uptake GO compared to pristine graphene, since the latter remains blocked on the cell surface, probably because it is poorly dispersed in water.[68,72] It was reported that at 50 μg mL^{-1}, pristine graphene induces macrophage apoptosis, while below this concentration it triggers cytokine release and impairs macrophage function.[68,83,84] Ingested GO sheets form aggregates in macrophage cytoplasm[80,85] and induce the production of proinflammatory cytokines.[72,75,80] Macrophage phagocytosis depends on GO lateral size; large sheets can align with the membranes of cells and develop a "masking" effect isolating cells from the environment.[86] This effect is similar to the "wrapping" effect on bacterial cells that causes their isolation and consequent growth inhibition.[19] Large GO sheets (750–1330 nm), in comparison with their smaller counterparts (50–350 nm), can induce M1 macrophage polarization, NF-κB activation and the production of proinflammatory cytokines.[87]

A direct comparison of the effect of materials with similar dispersibility but different oxidation states (GO and rGO nanoplatelets with size <100 nm) was conducted for monocytes and macrophage precursors (Fig. 5). GO nanoparticles have been obtained with the modified Hummers' method and sonication, while rGO was obtained via UV photoreduction of the former.[88] rGO is better ingested in respect to GO but induces differential expression patterns of antioxidative enzymes. The effects of exposed THP-1 cells could also pass to THP-1a as shown in Fig. 5, reproduced from ref. 88 GO nanoparticles (GONPs) demonstrated a stronger inhibition of THP-1a phagocytosis towards E. coli as compared to rGO nanoparticles (rGONPs) and both GONPs and rGONPs impaired the phagocytosis and endocytosis abilities of THP-1a.

Concerning the BC effect, phagocytosis by macrophages seems to be mediated by the Fcγ receptor that recognizes GO opsonized by IgG.[75] Surface modification of GO with PEG reduces IgG enrichment in the GO corona, and consequently inhibits macrophage phagocytosis and improves biocompatibility. However, it should also be kept in mind that other proteins (such as complement C4, serotransferrin or unknown proteins) might also cause specific ligand–receptor interactions and affect the circulation time of functionalized GO.[56]

Other important phagocytic cells are dendritic cells (DC) that activate antigen-specific T cells, after (i) antigen capture, (ii) intracellular processing and (iii) the presentation of the antigen within the MHC complex on the cell surface.

The maturation of DC is induced significantly by GO in a dose-dependent fashion, as reflected by the up-regulation of
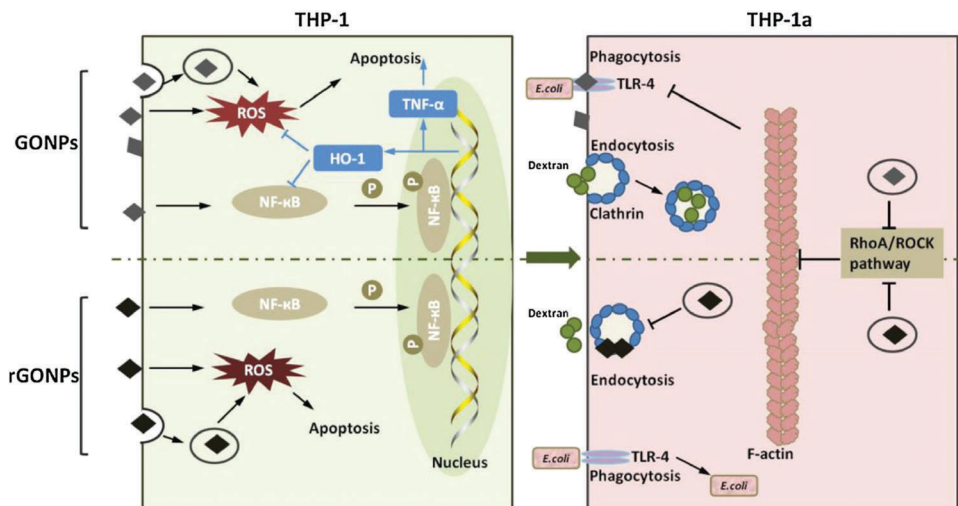
Fig. 5 Illustration of the short-term effects of GONPs and rGONPs on THP-1 cells, and the long-term effects on THP-1a differentiation from THP-1 cells. GONPs and rGONPs could have induced ROS formation and activated the NF-κB pathway in THP-1 cells. rGONPs could not fully transcript proinflammatory genes due to lack of additional transcription factors. Reproduced with permission from ref. 72.

surface receptor phenotypes.[85,89] However, the GO-treated DC failed to correctly present antigens to lymphocytes (Fig. 3-2e). The uptake of antigens is not altered but GO interacts directly with the subunit LMP7 of the immunoproteasome responsible for antigen processing.[89]

Below 50 μg mL^{-1}, T lymphocyte vitality is not affected by GO or GO-COOH, a GO enriched with carboxyl.[39] Above this concentration, vitality is reduced. Apoptosis seems to be induced by an external mechanism, without internalization, via ROS-dependent/independent signaling for GO-COOH and GO respectively. Despite apoptosis induction, both nanomaterials do not interfere with lymphocyte immune response ability. It should be noted that when cells are treated with GO or GO-COOH and the cell medium does not contain FBS, the cytotoxicity is dramatically higher, indicating the formation of a protecting BC around the nanomaterials.[39] T lymphocyte apoptosis after treatment with GO was reported to be higher (∼70% at 100 μg mL^{-1}) by Zhi and colleagues.[85]

A series of safety guidelines for the development of graphene-based materials for in vivo applications like the use of small, well-dispersed sheets that macrophages can efficiently phagocytize, and the use of degradable GBM have been proposed.[90] On the other hand, GO immunostimulatory activity and high surface area for antigen adsorption have encouraged studies on GO usage as an adjuvant in vaccine therapy.[91,92] Meng and colleagues explored the potential of ovalbumin and carnosine functionalized GO to promote specific antibody response and increase lymphocyte proliferation efficiency and T-cell activation.[91] GO functionalized with both PEG and poly-ethyleneimine (PEI), GO-PEG-PEI, can represent an innovative method for the delivery of urease B antigen, specific for Helicobacter pylori to dendritic cells. GO-PEG-PEI significantly enhances the maturation of DCs that release interleukin 12 (IL-12) through the activation of multiple Toll-like receptors (TLRs).[92]

6. Biodistribution and biosafety of GO: future challenges

The focus of this review is the GO interaction with blood components and BC in light of the future design of GO pharmaceutical delivery systems. Intravenously injected drug delivery systems (DDS) developed so far include PEGylated nanographene sheets for tumor passive targeting,[93] rGO functionalized with chitosan and iron oxide magnetic nanoparticles for the delivery of doxorubicin[94] and epidermal growth factor receptor antibody-conjugated PEGylated nanographene oxide for epirubicin delivery in tumors[55] (for a comprehensive outlook of DDS based on graphene see ref. 95). Nanoparticles intended for drug delivery applications are being engineered to reduce their clearance and extend systemic circulation times and thus increase the opportunity for targeted delivery. However, the disadvantage of prolonged circulation times is the greater chance of interaction with blood components and activation of adverse effects.

Before any nanomaterial translation into clinical therapy, there are biosafety concerns that need to be addressed. We have seen how GO interacts with blood system components and how BC can influence these interactions, but what is the biodistribution and the toxicity when GO is administered intravenously (i.v.)?

Studies have reported inconsistencies in GO effects in vivo, as summarized in recent reviews.[90,96–98]

The early study of Zhang and colleagues determined the distribution and biocompatibility of i.v. injected GO in mice.[99] The half-life of GO in blood is much longer than in other carbon nanomaterials (∼5 hours). Within 48 hours after i.v. injection, GO is cleared from the bloodstream and distributed throughout various organs with preferred accumulation in the lungs, liver, and spleen. The lack of pathological changes was reported after 14 days of treatment at a low dose (1 mg kg^{-1}),

but at a higher dose (10 mg kg^{-1}), granulomatous lesions, pulmonary edema, inflammatory cell infiltration, and fibrosis throughout the lung were observed.[99] Many studies confirmed that the primary site of GO accumulation and toxicity *in vivo* is the lungs.[97] It seems that the pathological effects on the lungs are proportional to the degree of dispersion and oxidation of GO. When directly injected into the lungs, GO induces severe long-term (21 days) lung injury, while graphene flakes, either in a dispersed or aggregated state, do not increase apoptosis in lung macrophages.[100] The biodistribution of GO is size-dependent. In the report by Zhang, the size of GO ranged from 10 to 800 nm and that this caused a distinctive clearance behavior: particles with small size were quickly eliminated through the renal route within 12 h post injection, while large particles were intercepted by the lungs.[99] A systematic study on GO size, dose and dosing frequency was conducted by Liu and colleagues.[58] Liu intravenously administered two types of GO: small GO flakes (s-GO, average hydrodynamic diameter of $\sim$250 nm) and large GO flakes (l-GO, average hydrodynamic diameter of $\sim$900 nm) at a single high dose (2.1 mg kg^{-1}) or seven repeated low doses (0.3 mg kg^{-1}); irrespective of size, the single high-dose administration of GO induced lung damage and infiltration of inflammatory cells. In the lungs, GO accumulated in the macrophages but not in the lymphocytes, which were recruited but were not able to trap GO. In this study, the authors claimed that although oxidative stress is a widely existent phenomenon in cells exposed *in vitro* to GO, the protective effect of proteins forming a BC around GO should be considered *in vivo*.

Interesting size-dependent results were reported for multiple-dose exposure. The s-GO did not induce renal damage or accumulate in the kidneys since it was quickly eliminated through the glomeruli. Conversely, l-GO failed to be cleared through kidneys and induced damage. The lungs were damaged only after multiple doses of l-GO. This effect depends on the aggregation of GO with proteins that induce the blockage of large GO-complexes in the lungs. The hypothesis relies on the formation of multiple complexes of l-GO and proteins that enter the capillaries and create multiple injury points and inflammatory cell recruitment. s-GO could instead pass through lungs capillaries after each low-dose administration. The kidneys and lungs were more damaged by l-GO, while the s-GO preferentially accumulated in the liver with toxic effects.

At a high single dose, s-GO can also damage the lungs since at high concentration it forms large complexes that reach a similar size to the l-GO protein complex.[44]

In summary, s-GO is safer than l-GO, but at a single high dose the aggregation with blood proteins, and therefore the BC, induces the formation of toxic large complexes. These results are in accordance with the study by Qu and colleagues, in which GO (30–1000 nm) aggregation was suppressed with the addition of Tween-80 surfactant.[101] While GO aggregated and accumulated in the lung macrophages, Tween-80 GO was more stable and accumulated in the liver inside Kuppfer cells (macrophages).[101] Interestingly, rGO seems to have reduced thrombogenicity *in vivo*, improved biocompatibility and brain tissue targeting.[63,77,102]

The intravenous administration of rGO (with a lateral size of 342 nm administered at 7 mg kg^{-1} in a single dose) led to minor signs of toxicity in the blood, liver and kidneys and a lack of inflammation after 7 days.

It is known that the adsorption of BC is a key factor affecting the biodistribution of nanoparticles. The BC can act in two ways: (i) promoting/avoiding the ingestion of phagocytic cells and influencing circulating time; (ii) regulating the size of nanomaterials. Size regulates distribution, and particles with size smaller than capillaries are phagocytized mainly in the liver, spleen and bone marrow; conversely, large particles are trapped in the lungs.[44]

GO therefore follows the rules of size distribution as other nanomaterials. However, the BC also influences the uptake by the immune cells both in the bloodstream (by monocytes, platelets, leukocytes, and dendritic cells) and in tissues by resident phagocytes (*e.g.*, Kupffer cells in the liver, DC in lymph nodes, macrophages and B cells in the spleen). IgG and complement proteins in the protein corona help to reorganize nanoparticles in immune cells and reticuloendothelial system organs.[59] Conversely, the macrophage uptake can be reduced by maintaining the particle size at $\sim$150 nm and by conferring the nanomaterial with hydrophilic molecules or albumin that reduce the opsonin interactions[59,98] and non-specific protein adsorption.[103]

The addition of polymer coatings such as PEG to the nanomaterial surface is a tool for avoiding recognition by the immune cells. PEG is known to prolong particle circulation in the blood and significantly decrease uptake by the spleen and liver-resident phagocytes. It has been hypothesized that PEG creates a steric shield around the coated particle, effectively preventing plasma proteins from adhering to the particle surface and thus avoiding subsequent uptake by mononuclear phagocytes. PEGylated GO sheets (10–30 nm) were reported to be mainly distributed in the liver and spleen and did not exhibit toxicity at high doses (20 mg kg^{-1}) within 90 days.[74,104] This was likely due to both the small size and PEGylation, which stabilized the nanomaterial and prevented the aggregation as well as reduced the BC formation.

Luo and colleagues demonstrated that PEGylation of GO does not prevent macrophage activation.[105] nGO-PEG, a functionalized GO with a lateral size of $\sim$200 nm, prevents macrophages uptake, but through physical contact with their cell membranes, boosts the release of cytokines, potentially leading to further immunological responses downstream.

Like PEGylation, dextran coating is a well-known strategy to reduce the adsorption of proteins on nanomaterials and improve biocompatibility.[106,107] Dextran-GO, obtained with a protocol of covalent conjugation, showed rapid clearance from the blood, accumulation in the liver and spleen and elimination from the bodies of the mice after a week.[106]

As we have seen in Section 3, the surface functionalization of GO can modify its protein corona. The GO-PAA, can reduce the organ impairments in the liver and lung with respect to GO-, GO-NH$_2$, GO-PAM and GO-PEG-treated mice.[56]

Finally, the degradation of injected GO is an important biosafety concern. Long-term interaction (14 days) of GO with

plasma causes reduction and biodegradation with hole formation caused by the action of hydroxyl radicals.[54] Once internalized by the immune cells, biodegradable particles are digested and cleared from the body, while non-biodegradable particles accumulate in cells for extended periods.

A recent study investigated the degradation of large GO (10 µm) and small GO (100 nm) by neutrophils myeloperoxidase (MPO).[108] Both kinds of GO sheets were degraded within 12 hours by recombinant human MPO as well as neutrophils after degranulation. Furthermore, the products of the reaction were tested for toxicity on a human bronchial epithelial cell line and demonstrated to be safe. It seems, however, that MPO degradation is highly dependent on GO stability and that aggregated GO sheets fail to undergo degradation. Further studies should confirm neutrophil efficacy in GO disposal *in vivo*.[109] Others reported that macrophages are instead primarily involved in the degradation of carboxylated graphene *in vivo*.[110]

Although PEGylation reduces GO toxicity, it can hinder the GO degradation. Both PEG or BSA coated GO/rGO are resistant to enzyme horseradish peroxidase (HRP) digestion. In the same study, Li and colleagues conjugated PEG to GO *via* a cleavable disulfide bond (GO-SS-PEG) and improved the degradability of nanoparticles that after reaching the designated tissues may undergo cleavage of disulfide bonds by glutathione in the cell cytoplasm/the myeloperoxidase in the phagosomes of phagocytes.[74]

Despite the great scientific advances, future studies for *in vivo* application should focus on some weaknesses in graphene research. First, graphene materials should be designed to have more than just a stable small size for rapid excretion, and degradable composition to limit toxicity. Detailed physico-chemical characterization, including size, surface area, charge, purity, oxygen content, stability in body fluids and the composition of the BC, should be described in papers aimed at the pharmacological administration of graphene.

In 2017, Reina and colleagues defined guidelines for the development of a clearer picture of the toxicity of graphene-based materials to accelerate the transition of scientific results into clinics.[111] These guidelines can be summarized as follows:

– use of the established nomenclature for the material

– provide physicochemical characterization (C/O ratio, surface modification/functionalization, metal traces, size, the number of layers, surface area, surface charge *etc.*) and manu-facturing information

– use the recommended processing methods

– perform biocompatibility tests, cytotoxicity, genotoxicity, biodegradation, distribution and accumulation into organs, metabolism.

The BC forms in cell culture medium when FBS is present and this influences the *in vitro* results. This and the peculiar graphene optical properties might influence standard biological assays like the MTT (3-(4,5-dimethylthiazol-2-yl)-2,5-diphenyl-tetrazolium bromide) assay for cell metabolism and should be considered when GO is tested *in vitro*. It is also possible that GO, thanks to its high-protein binding properties, can block some reagents used in the biological assays.[8] Dedicated protocols should be established by the scientific community.[112]

7. Conclusions

In the last decade, the design of injectable nanoparticles has affected the control of the BC formation, the interface seen by cells and tissues, *in vivo*. Combining all the experimental results presented in this review, we can conclude that the BC significantly affects several interactions of GO. The BC inhibits the hemolytic effects of GO, regulates complement activation, and mediates immune response activity and biodistribution.

Given the difficulty of precisely controlling the *in vivo* interaction with proteins, most of the strategies designed to modulate the BC are based on functionalization with anti-fouling polymeric residues that suppress protein adsorption, altogether lowering the targeting efficiency.[43] In the case of GO, pre-coating with chitosan to reduce non-specific protein adsorption, functionalization with dextran or PEG to improve elimination from the body or modification of surface func-tional groups by amination and carboxylation are examples of approaches to modulating the BC.

One can imagine that unique nanomaterial BC properties might be useful for specific cell targeting application. The BC compositions of GO and rGO have just started to be studied, but the first data are encouraging. As an example, ApoE residue enrichment of the graphene corona can be useful for over-coming the blood–brain barrier and targeting the cerebrovas-cular endothelium for neurological disease treatment.[113] GO complement activation can, in turn, be exploited for enhanced antigen presentation in vaccines when administered *via* other routes, *e.g.*, subcutaneously or intradermally.[8] GO accumula-tion in lungs can be exploited for the passive pulmonary delivery of pharmaceuticals.[114]

Furthermore, GO-BC displays unique features when submerged in plasma with patients having diseases like diabetes, and can be exploitable to develop BC-based diagnostic methods.[52,115] Future studies should precisely describe the relationship between GO oxidation, size and dispersibility and BC properties obtained after incubation in serum or plasma. Another important unaddressed question is how the corona might influence the biocompatibility of the graphene-based bioengineering solid implants, considering the variability of BC composition when scaffolds are implanted in patients.[116]

Based on the great advances in GO research, we can foresee that new opportunities in nanomedical applications will be available. We hope that the arguments presented in this review will help researchers in moving forward and pushing the limits of GO toward clinical applications.

List of abbreviations

AFM	Atomic force microscopy
ApoA-1	Apolipoprotein A-1
ApoE	Apolipoprotein E

BBB	Blood–brain barrier
BC	Biomolecular corona
BFG	Bovine fibrinogen
BSA	Bovine serum protein
BSA-g-RGO	BSA grafted polydopamine rGO
CB	Carbon black
CNT-COOH	Carboxylic-functionalized multi-walled CNT
CS	Chitosan
DA	Dopamine
DC	Dendritic cells
DDS	Drug delivery systems
FBS	Foetal bovine serum
FLG	Few-layer graphene
G-BC	Biomolecular corona of graphene
GBM	Graphene-based materials
G-NH$_2$	Aminated rGO
GNPs	Graphene nanoplatelets
GO	Graphene oxide
GONPs	GO nanoparticles
GO-PAA	GO-polyacrylic acid
GO-PAM	GO-polyacrylamide
GO-PEG	GO-polyethylene glycol
GO-PEG-PEI	GO-polyethylene glycol-polyethyleneimine
GO-SS-PEG	PEG conjugated to GO via a cleavable disulfide bond
Hep-gpRGO	Heparin-grafted polydopamine rGO
HRP	Horseradish peroxidase
HSA	Human serum albumin
Ig	Immunoglobulin
IgG	Immunoglobulin g
i.v.	Intravenously
LPS	Lipopolysaccharide
LS	Lateral size
MD	Molecular dynamics
MPO	Myeloperoxidase
MTT	3-(4,5-Dimethylthiazol-2-yl)-2,5-diphenyltetrazolium bromide
MWCNT	Multi-walled carbon nanotubes
PBS	Phosphate buffered saline
PBMC	Peripheral blood mononuclear cells
PEG	Polyethylene glycol
PEI	Polyethyleneimine
PGO	Porous graphene oxide
Phe	Phenylalanine
polyDA-rGO	rGO functionalized with DA
RBCs	Red blood cells
rGO	Reduced graphene oxide
rGONPs	rGO nanoparticles
SWCNT	Single-walled carbon nanotubes
Tf	Transferrin
Trp	Tryptophan
Tyr	Tyrosine

Conflicts of interest

There are no conflicts to declare.

References

1 A. N. Banerjee, Graphene and its derivatives as biomedical materials, future prospects and challenges, *Interface Focus*, 2018, **8**(3), 20170056.

2 C. K. Chua and M. Pumera, Chemical reduction of graphene oxide, a synthetic chemistry viewpoint, *Chem. Soc. Rev.*, 2014, **43**(1), 291–312.

3 A. Bianco, H. Cheng, T. Enoki, Y. Gogotsi, R. H. Hurt, N. Koratkar, T. Kyotani, M. Monthioux, C. R. Park, J. M. D. Tascon and J. Zhang, All in the graphene family – a recommended nomenclature for two-dimensional carbon materials, *Carbon*, 2013, **65**, 1–6.

4 S. Pei and H. M. Cheng, The reduction of graphene oxide, *Carbon*, 2012, **50**(9), 3210–3228.

5 J. P. M. Almeida, A. L. Chen, A. Foster and R. Drezek, In vivo biodistribution of nanoparticles, *Nanomedicine*, 2011, **6**(5), 815–835.

6 Kenry, K. P. Loh and C. T. Lim, Molecular interactions of graphene oxide with human blood plasma proteins, *Nanoscale*, 2016, **8**(17), 9425–9441.

7 D. Caputo, M. Papi, R. Coppola, S. Palchetti, L. Digiacomo, G. Caracciolo and D. Pozzi, A protein corona-enabled blood test for early cancer detection, *Nanoscale*, 2017, **9**(1), 349–354.

8 M. A. Dobrovolskaia, P. Aggarwal, J. B. Hall and S. E. McNeil, Preclinical studies to understand nanoparticle interaction with the immune system and its potential effects on nanoparticle biodistribution, *Mol. Pharmaceutics*, 2008, **5**(4), 487–495.

9 Y. Zhang, C. Wu, S. Guo and J. Zhang, Interactions of graphene and graphene oxide with proteins and peptides, *Nanotechnol. Rev.*, 2013, **2**(1), 27–45.

10 D. F. Báez, H. Pardo, I. Laborda, J. F. Marco, C. Yáñez and S. Bollo, Reduced graphene oxides, Influence of the reduction method on the electrocatalytic effect towards nucleic acid oxidation, *Nanomaterials*, 2017, **7**(7), 168, DOI: 10.3390/nano7070168.

11 D. R. Dreyer, A. D. Todd and C. W. Bielawski, Harnessing the chemistry of graphene oxide, *Chem. Soc. Rev.*, 2014, **43**(15), 5288–5301.

12 M. Simsikova and T. Sikola, Interaction of Graphene Oxide with Proteins and Applications of their Conjugates, *J. Nanomed. Res.*, 2017, **5**(2), 00109.

13 J. Yang, K. Y. Hsieh, P. V. Kumar, S. Cheng, Y. Lin, Y. Shen and G. Chen, Enhanced Osteogenic Differentiation of Stem Cells on Phase-Engineered Graphene Oxide, *ACS Appl. Mater. Interfaces*, 2018, **10**(15), 12497–12503.

14 W. Hu, C. Peng, M. Lv, X. Li, Y. Zhang, N. Chen, C. Fan and Q. Huang, Protein corona-mediated mitigation of cytotoxicity of graphene oxide, *ACS Nano*, 2011, **5**(5), 3693–3700.

15 J. Zhang, H. Yang, G. Shen, P. Cheng, J. Zhang and S. Guo, Reduction of graphene oxide *via* L-ascorbic acid, *Chem. Commun.*, 2010, **46**(7), 1112–1114.

16 A. G. Marrani, A. C. Coico, D. Giacco, R. Zanoni, F. A. Scaramuzzo, R. Schrebler, D. Dinia, M. Bonomoa and E. A. Dalchieled, Integration of graphene onto silicon through electrochemical reduction of graphene oxide layers in non-aqueous medium, *Appl. Surf. Sci.*, 2018, **445**, 404–414.

17 I. Chowdhury, N. D. Mansukhani, L. M. Guiney, M. C. Hersam and D. Bouchard, Aggregation and stability of reduced graphene oxide, complex roles of divalent cations, pH, and natural organic matter, *Environ. Sci. Technol.*, 2015, **49**(18), 10886–10893.

18 M. Orecchioni, C. Ménard-Moyon, L. G. Delogu and A. Bianco, Graphene and the immune system, challenges and potentiality, *Adv. Drug Delivery Rev.*, 2016, **105**, 163–175.

19 V. Palmieri, M. C. Lauriola, G. Ciasca, C. Conti, M. De Spirito and M. Papi, The graphene oxide contradictory effects against human pathogens, *Nanotechnology*, 2017, **15**, 152001, DOI: 10.1088/1361-6528/aa6150.

20 M. Papi, V. Palmieri, F. Bugli, M. De Spirito, M. Sanguinetti, C. Ciancico, M. C. Braidotti, S. Gentilini, L. Angelani and C. Conti, Biomimetic antimicrobial cloak by graphene-oxide agar hydrogel, *Sci. Rep.*, 2016, **6**(1), 12, DOI: 10.1038/s41598-016-0010-7.

21 D. Li, W. Zhang, X. Yu, Z. Wang, Z. Su and G. Wei, When biomolecules meet graphene from molecular level interactions to material design and applications, *Nanoscale*, 2016, **8**(47), 19491–19509.

22 D. Y. Lee, Z. Khatun, J. Lee, Y. Lee and I. In, Blood compatible graphene/heparin conjugate through noncovalent chemistry, *Biomacromolecules*, 2011, **12**(2), 336–341.

23 M. Hassan, M. Walter and M. Moseler, Interactions of polymers with reduced graphene oxide, van der Waals binding energies of benzene on graphene with defects, *Phys. Chem. Chem. Phys.*, 2014, **16**(1), 33–37.

24 L. Baweja, K. Balamurugan, V. Subramanian and A. Dhawan, Effect of graphene oxide on the conformational transitions of amyloid beta peptide, A molecular dynamics simulation study, *J. Mol. Graphics Modell.*, 2015, **61**, 175–185.

25 Y. Chong, C. Ge, Z. Yang, J. A. Garate, Z. Gu, J. K. Weber, L. Jiajia and Z. Ruhong, Reduced cytotoxicity of graphene nanosheets mediated by blood-protein coating, *ACS Nano*, 2015, **9**(6), 5713–5724.

26 J. N. Belling, J. A. Jackman, S. Yorulmaz Avsar, J. H. Park, Y. Wang, M. G. Potroz, A. R. Ferhan, P. S. Weiss and N. J. Cho, Stealth immune properties of graphene oxide enabled by surface-bound complement factor H, *ACS Nano*, 2016, **10**(11), 10161–10172.

27 H. Sun, A. Varzi, V. Pellegrini, D. Dinh, R. Raccichini, A. Del Rio-Castillo, M. Prato, M. Colombo, R. Cingolani, B. Scrosati, S. Passerini and F. Bonaccorso, How much does size really matter? Exploring the limits of graphene as Li ion battery anode material, *Solid State Commun.*, 2017, **251**, 88–93.

28 S. Li, A. N. Aphale, I. G. Macwan, P. K. Patra, W. G. Gonzalez, J. Miksovska and R. M. Leblanc, Graphene oxide as a quencher for fluorescent assay of amino acids, peptides, and proteins, *ACS Appl. Mater. Interfaces*, 2012, **4**(12), 7069–7075.

29 Kenry, Understanding the hemotoxicity of graphene nanomaterials through their interactions with blood proteins and cells, *J. Mater. Res.*, 2018, **33**(1), 44–57.

30 Z. Ding, H. Ma and Y. Chen, Interaction of graphene oxide with human serum albumin and its mechanism, *RSC Adv.*, 2014, **4**(98), 55290–55295.

31 X. Wu, Y. Xing, K. Zeng, K. Huber and J. X. Zhao, Study of Fluorescence Quenching Ability of Graphene Oxide with a Layer of Rigid and Tunable Silica Spacer, *Langmuir*, 2018, **34**(2), 603–611.

32 Kenry, K. P. Loh and C. T. Lim, Selective concentration-dependent manipulation of intrinsic fluorescence of plasma proteins by graphene oxide nanosheets, *RSC Adv.*, 2016, **6**(52), 46558–46566.

33 V. Palmieri, F. Bugli, M. C. Lauriola, M. Cacaci, R. Torelli, G. Ciasca, C. Conti, M. Sanguinetti, M. Papi and M. De Spirito, Bacteria Meet Graphene, Modulation of Graphene Oxide Nanosheet Interaction with Human Pathogens for Effective Antimicrobial Therapy, *ACS Biomater. Sci. Eng.*, 2017, **3**(4), 619–627.

34 J. Kuchlyan, N. Kundu, D. Banik, A. Roy and N. Sarkar, Spectroscopy and fluorescence lifetime imaging microscopy to probe the interaction of bovine serum albumin with graphene oxide, *Langmuir*, 2015, **31**(51), 13793–13801.

35 S. S. K. Mallineni, J. Shannahan, A. J. Raghavendra, A. M. Rao, J. M. Brown and R. Podila, Biomolecular Interactions and Biological Responses of Emerging Two-Dimensional Materials and Aromatic Amino Acid Complexes, *ACS Appl. Mater. Interfaces*, 2016, **8**(26), 16604–16611.

36 H. Vovusha, S. Sanyal and B. Sanyal, Interaction of nucleobases and aromatic amino acids with graphene oxide and graphene flakes, *J. Phys. Chem. Lett.*, 2013, **4**(21), 3710–3718.

37 Z. Gu, Z. Yang, L. Wang, H. Zhou, C. A. Jimenez-Cruz and R. Zhou, The role of basic residues in the adsorption of blood proteins onto the graphene surface, *Sci. Rep.*, 2015, **5**, 10873.

38 L. Baweja, K. Balamurugan, V. Subramanian and A. Dhawan, Hydration patterns of graphene-based nanomaterials (GBNMs) play a major role in the stability of a helical protein, a molecular dynamics simulation study, *Langmuir*, 2013, **29**(46), 14230–14238.

39 Z. Ding, Z. Zhang, H. Ma and Y. Chen, *In vitro* hemocompatibility and toxic mechanism of graphene oxide on human peripheral blood T lymphocytes and serum albumin, *ACS Appl. Mater. Interfaces*, 2014, **6**(22), 19797–19807.

40 Kenry, A. Geldert, Y. Liu, K. P. Loh and C. T. Lim, Nano–bio interactions between carbon nanomaterials and blood plasma proteins, why oxygen functionality matters, *NPG Asia Mater.*, 2017, **9**(8), e422.

41 P. P. Karmali and D. Simberg, Interactions of nanoparticles with plasma proteins, implication on clearance

and toxicity of drug delivery systems, *Expert Opin. Drug Delivery*, 2011, **8**(3), 343–357.

42 V. Pareek, A. Bhargava, V. Bhanot, R. Gupta, N. Jain and J. Panwar, Formation and Characterization of Protein Corona Around Nanoparticles, A Review, *Nanosci. Nanotechnol.*, 2018, **18**, 6653–6670.

43 C. D. Walkey and W. C. Chan, Understanding and controlling the interaction of nanomaterials with proteins in a physiological environment, *Chem. Soc. Rev.*, 2012, **41**(7), 2780–2799.

44 J. Liu, S. Yang, H. Wang, Y. Chang, A. Cao and Y. Liu, Effect of size and dose on the biodistribution of graphene oxide in mice, *Nanomedicine*, 2012, **7**(12), 1801–1812.

45 H. Mao, W. Chen, S. Laurent, C. Thirifays, C. Burtea, F. Rezaee and M. Mahmoudi, Hard corona composition and cellular toxicities of the graphene sheets, *Colloids Surf., B*, 2013, **109**, 212–218.

46 V. Castagnola, W. Zhao, L. Boselli, M. L. Giudice, F. Meder, E. Polo, K. R. Paton, C. Backes, J. N. Coleman and K. A. Dawson, Biological recognition of graphene nanoflakes, *Nat. Commun.*, 2018, **9**(1), 1577.

47 L. Digiacomo, F. Cardarelli, D. Pozzi, S. Palchetti, M. Digman, E. Gratton, A. L. Capriotti, M. Mahmoudi and G. Caracciolo, An apolipoprotein-enriched biomolecular corona switches the cellular uptake mechanism and trafficking pathway of lipid nanoparticles, *Nanoscale*, 2017, **9**(44), 17254–17262.

48 V. Mirshafiee, R. Kim, M. Mahmoudi and M. L. Kraft, The importance of selecting a proper biological milieu for protein corona analysis *in vitro*, Human plasma *versus* human serum, *Int. J. Biochem. Cell Biol.*, 2016, **75**, 188–195.

49 M. Sopotnik, A. Leonardi, I. Križaj, P. Dušak, D. Makovec, T. Mesarič, N. P. Ulrih, I. Junkar, K. Sepčić and D. Drobne, Comparative study of serum protein binding to three different carbon-based nanomaterials, *Carbon*, 2015, **95**, 560–572.

50 X. Wei, L. Hao, X. Shao, Q. Zhang, X. Jia, Z. R. Zhang, Y. F. Lin and Q. Peng, Insight into the interaction of graphene oxide with serum proteins and the impact of the degree of reduction and concentration, *ACS Appl. Mater. Interfaces*, 2015, **7**(24), 13367–13374.

51 Z. Gu, Z. Yang, Y. Chong, C. Ge, J. K. Weber, D. R. Belland and R. Zhou, Surface curvature relation to protein adsorption for carbon-based nanomaterials, *Sci. Rep.*, 2015, **5**, 10886.

52 M. J. Hajipour, J. Raheb, O. Akhavan, S. Arjmand, O. Mashinchian, M. Rahman, M. Abdolahad, V. Serpooshan, S. Laurent and M. Mahmoudi, Personalized disease-specific protein corona influences the therapeutic impact of graphene oxide, *Nanoscale*, 2015, **7**(19), 8978–8994.

53 G. Caracciolo, O. C. Farokhzad and M. Mahmoudi, Biological identity of nanoparticles *in vivo*, clinical implications of the protein corona, *Trends Biotechnol.*, 2017, **35**(3), 257–264.

54 X. Hu, D. Li and L. Mu, Biotransformation of graphene oxide nanosheets in blood plasma affects their interactions with cells, *Environ. Sci.: Nano*, 2017, **4**(7), 1569–1578.

55 X. Tan, L. Feng, J. Zhang, K. Yang, S. Zhang, Z. Liu and R. Peng, Functionalization of graphene oxide generates a unique interface for selective serum protein interactions, *ACS Appl. Mater. Interfaces*, 2013, **5**(4), 1370–1377.

56 M. Xu, J. Zhu, F. Wang, Y. Xiong, Y. Wu, Q. Wang, J. Weng, Z. Zhang, W. Chen and S. Liu, Improved *in vitro* and *in vivo* biocompatibility of graphene oxide through surface modification, poly(acrylic acid)-functionalization is superior to PEGylation, *ACS Nano*, 2016, **10**(3), 3267–3281.

57 T. Yan, H. Zhang, D. Huang, S. Feng, M. Fujita and X. D. Gao, Chitosan-functionalized graphene oxide as a potential immunoadjuvant, *Nanomaterials*, 2017, **7**(3), 59.

58 J. H. Liu, T. Wang, H. Wang, Y. Gu, Y. Xu, H. Tang, G. Jiae and Y. Liu, Biocompatibility of graphene oxide intravenously administrated in mice—effects of dose, size and exposure protocols, *Toxicol. Res.*, 2015, **4**(1), 83–91.

59 P. Aggarwal, J. B. Hall, C. B. McLeland, M. A. Dobrovolskaia and S. E. McNeil, Nanoparticle interaction with plasma proteins as it relates to particle biodistribution, biocompatibility and therapeutic efficacy, *Adv. Drug Delivery Rev.*, 2009, **61**(6), 428–437.

60 A. Moore, R. Weissleder and J. A. Bogdanov, Uptake of dextran-coated monocrystalline iron oxides in tumor cells and macrophages, *J. Magn. Reson. Imaging*, 1997, **7**(6), 1140–1145.

61 A. Zoubeidi, K. Chi and M. Gleave, Targeting the cytoprotective chaperone, clusterin, for treatment of advanced cancer, *Clin. Cancer Res.*, 2010, **16**(4), 1088–1093.

62 C. H. Stuart, K. R. Riley, O. Boyacioglu, D. M. Herpai, W. Debinski, S. Qasem, F. C. Marini, C. L. Colyer and W. H. Gmeiner, Selection of a Novel Aptamer Against Vitronectin Using Capillary Electrophoresis and Next Generation Sequencing, *Mol. Ther.–Nucleic Acids*, 2016, **5**(11), e386.

63 M. C. P. Mendonça, E. S. Soares, M. B. de Jesus, H. J. Ceragioli, M. S. Ferreira, R. R. Catharino and M. A. da Cruz-Höfling, Reduced graphene oxide induces transient blood–brain barrier opening, an *in vivo* study, *J. Nanobiotechnol.*, 2015, **13**(1), 78.

64 R. Feng, Y. Yu, C. Shen, Y. Jiao and C. Zhou, Impact of graphene oxide on the structure and function of important multiple blood components by a dose-dependent pattern, *J. Biomed. Mater. Res., Part A*, 2015, **103**(6), 2006–2014.

65 S. K. Singh, M. K. Singh, P. P. Kulkarni, V. K. Sonkar, J. J. Grácio and D. Dash, Amine-modified graphene, thrombo-protective safer alternative to graphene oxide for biomedical applications, *ACS Nano*, 2012, **6**(3), 2731–2740.

66 K. H. Liao, Y. S. Lin, C. W. Macosko and C. L. Haynes, Cytotoxicity of graphene oxide and graphene in human erythrocytes and skin fibroblasts, *ACS Appl. Mater. Interfaces*, 2011, **3**(7), 2607–2615.

67 M. Papi, M. Lauriola, V. Palmieri, G. Ciasca, G. Maulucci and D. Spirito, Plasma protein corona reduces the haemolytic activity of graphene oxide nano and micro flakes, *RSC Adv.*, 2015, **5**(99), 81638–81641.

68 A. Sasidharan, L. S. Panchakarla, A. R. Sadanandan, A. Ashokan, P. Chandran, C. M. Girish, D. Menon, S. V. Nair, C. N. Rao and M. Koyakutty, Hemocompatibility and macrophage response of pristine and functionalized graphene, *Small*, 2012, **8**(8), 1251–1263.

69 S. M. Chowdhury, S. Kanakia, J. D. Toussaint, M. D. Frame, A. M. Dewar, K. R. Shroyer, W. Moore and B. Sitharaman, *In vitro* hematological and *in vivo* vasoactivity assessment of dextran functionalized graphene, *Sci. Rep.*, 2013, **3**, 2584.

70 F. Bugli, M. Cacaci, V. Palmieri, R. Di Santo, R. Torelli, G. Ciasca, M. Di Vito, A. Vitali, C. Conti, M. Sanguinetti, M. De Spirito and M. Papi, Curcumin-loaded graphene oxide flakes as an effective antibacterial system against methicillin-resistant *Staphylococcus aureus*, *Interface Focus*, 2018, **8**(3), 20170059.

71 C. Cheng, S. Nie, S. Li, H. Peng, H. Yang, L. Ma, S. Sun and C. Zhao, Biopolymer functionalized reduced graphene oxide with enhanced biocompatibility *via* mussel inspired coatings/anchors, *J. Mater. Chem. B*, 2013, **1**(3), 265–275.

72 B. Zhang, P. Wei, Z. Zhou and T. Wei, Interactions of graphene with mammalian cells, molecular mechanisms and bio-medical insights, *Adv. Drug Delivery Rev.*, 2016, **105**, 145–162.

73 G. Duan, S. G. Kang, X. Tian, J. A. Garate, L. Zhao and C. Ge, C Protein corona mitigates the cytotoxicity of graphene oxide by reducing its physical interaction with cell membrane, *Nanoscale*, 2015, **7**(37), 15214–15224.

74 Y. Li, L. Feng, X. Shi, X. Wang, Y. Yang and K. Yang, Surface Coating-Dependent Cytotoxicity and Degradation of Graphene Derivatives, Towards the Design of Non-Toxic, Degradable Nano-Graphene, *Small*, 2014, **10**(8), 1544–1554.

75 H. Yue, W. Wei, Z. Yue, B. Wang, N. Luo and Y. Gao, *et al.*, The role of the lateral dimension of graphene oxide in the regulation of cellular responses, *Biomaterials*, 2012, **33**(16), 4013–4021.

76 A. N. Ilinskaya and M. A. Dobrovolskaia, Nanoparticles and the blood coagulation system. Part II, safety concerns, *Nanomedicine*, 2013, **8**(6), 969–981.

77 S. K. Singh, M. K. Singh, M. K. Nayak, S. Kumari, S. Shrivastava and J. J. Grácio, Thrombus inducing property of atomically thin graphene oxide sheets, *ACS Nano*, 2011, **5**(6), 4987–4996.

78 N. Kurantowicz, B. Strojny, E. Sawosz, S. Jaworski, M. Kutwin and M. Grodzik, Biodistribution of a high dose of diamond, graphite, and graphene oxide nanoparticles after multiple intraperitoneal injections in rats, *Nanoscale Res. Lett.*, 2015, **10**(1), 398.

79 P. P. Wibroe, S. V. Petersen, N. Bovet, B. W. Laursen and S. M. Moghimi, Soluble and immobilized graphene oxide activates complement system differently dependent on surface oxidation state, *Biomaterials*, 2016, **78**, 20–26.

80 S. P. Mukherjee, M. Bottini and B. Fadeel, Graphene and the immune system, A romance of many dimensions, *Front. Immunol.*, 2017, **8**, 673.

81 I. Dudek, M. Skoda, A. Jarosz and D. Szukiewicz, The molecular influence of graphene and graphene oxide on the immune system under *in vitro* and *in vivo* conditions, *Arch. Immunol. Ther. Exp.*, 2016, **64**(3), 195–215.

82 M. Orecchioni, D. A. Jasim, M. Pescatori, R. Manetti, C. Fozza, F. Sgarrella, D. Bedognetti, A. Bianco, K. Kostarelos and L. G. Delogu, Molecular and genomic impact of large and small lateral dimension graphene oxide sheets on human immune cells from healthy donors, *Adv. Healthcare Mater.*, 2016, **5**(2), 276–287.

83 Y. Li, Y. Liu, Y. Fu, T. Wei, L. Le Guyader, G. Gao, R. S. Liu, Y. Z. Chang and C. Chen, The triggering of apoptosis in macrophages by pristine graphene through the MAPK and TGF-beta signaling pathways, *Biomaterials*, 2012, **33**(2), 402–411.

84 H. Zhou, K. Zhao, W. Li, N. Yang, Y. Liu, C. Chen and T. Wei, The interactions between pristine graphene and macrophages and the production of cytokines/chemokines via TLR-and NF-κB-related signaling pathways, *Biomaterials*, 2012, **33**(29), 6933–6942.

85 X. Zhi, H. Fang, C. Bao, G. Shen, J. Zhang, K. Wang, S. Guo, T. Wan and D. Cui, The immunotoxicity of graphene oxides and the effect of PVP-coating, *Biomaterials*, 2013, **34**(21), 5254–5261.

86 J. Russier, E. Treossi, A. Scarsi, F. Perrozzi, H. Dumortier, L. Ottaviano, M. Meneghetti, V. Palermo and A. Bianco, Evidencing the mask effect of graphene oxide, a comparative study on primary human and murine phagocytic cells, *Nanoscale*, 2013, **5**(22), 11234–11247.

87 J. Ma, R. Liu, X. Wang, Q. Liu, Y. Chen, R. P. Valle, Y. Y. Zuo, T. Xia and S. Liu, Crucial role of lateral size for graphene oxide in activating macrophages and stimulating pro-inflammatory responses in cells and animals, *ACS Nano*, 2015, **9**(10), 10498–10515.

88 J. Yan, L. Chen, C. C. Huang, S. C. Lung, L. Yang, W. C. Wang, P. H. Lin, G. Suo and C. H. Lin, Consecutive evaluation of graphene oxide and reduced graphene oxide nanoplatelets immunotoxicity on monocytes, *Colloids Surf., B*, 2017, **153**, 300–309.

89 A. V. Tkach, N. Yanamala, S. Stanley, M. R. Shurin, G. V. Shurin, E. R. Kisin, A. R. Murray, S. Pareso, T. Khaliullin, G. P. Kotchey, V. Castranova, S. Mathur, B. Fadeel, A. Star, V. E. Kagan and A. A. Shvedova, Graphene oxide, but not fullerenes, targets immunoproteasomes and suppresses antigen presentation by dendritic cells, *Small*, 2013, **9**(9–10), 1686–1690.

90 C. Bussy, H. Ali-Boucetta and K. Kostarelos, Safety considerations for graphene, lessons learnt from carbon nanotubes, *Acc. Chem. Res.*, 2012, **46**(3), 692–701.

91 C. Meng, X. Zhi, C. Li, C. Li, Z. Chen, X. Qiu, C. Ding, L. Ma, H. Lu, D. Chen, G. Liu and D. Cui, Graphene oxides decorated with carnosine as an adjuvant to modulate innate immune and improve adaptive immunity *in vivo*, *ACS Nano*, 2016, **10**(2), 2203–2213.

92 L. Xu, J. Xiang, Y. Liu, J. Xu, Y. Luo, L. Feng, Z. Liu and R. Peng, Functionalized graphene oxide serves as a novel vaccine nano-adjuvant for robust stimulation of cellular immunity, *Nanoscale*, 2016, **8**(6), 3785–3795.

93 K. Yang, S. Zhang, G. Zhang, X. Sun, S. T. Lee and Z. Liu, Graphene in mice, ultrahigh in vivo tumor uptake and efficient photothermal therapy, *Nano Lett.*, 2010, **10**(9), 3318–3323.

94 C. Wang, S. Ravi, U. S. Garapati, M. Das, M. Howell, J. Mallela, S. Alwarapan, S. S. Mohapatra and S. Mohapatra, Multifunctional chitosan magnetic-graphene (CMG) nano-particles, a theranostic platform for tumor-targeted co-delivery of drugs, genes and MRI contrast agents, *J. Mater. Chem. B*, 2013, **1**(35), 4396–4405.

95 D. Iannazzo, A. Pistone, I. Ziccarelli and S. Galvagno, Graphene-based materials for application in pharmaceutical nanotechnology, *Fullerens, Graphenes and Nanotubes*, Elsevier, 2018, pp. 297–329.

96 T. P. D. Shareena, D. McShan, A. K. Dasmahapatra and P. B. Tchounwou, A Review on Graphene-Based Nano-materials in Biomedical Applications and Risks in Environment and Health, *Nano-Micro Lett.*, 2018, **10**(3), 53.

97 M. Ema, M. Gamo and K. Honda, A review of toxicity studies on graphene-based nanomaterials in laboratory animals, *Regul. Toxicol. Pharmacol.*, 2017, **85**, 7–24.

98 S. F. Kiew, L. V. Kiew, H. B. Lee, T. Imae and L. Y. Chung, Assessing biocompatibility of graphene oxide-based nano-carriers, a review, *J. Controlled Release*, 2016, **226**, 217–228.

99 X. Zhang, J. Yin, C. Peng, W. Hu, Z. Zhu, W. Li, C. Fan and Q. Huang, Distribution and biocompatibility studies of graphene oxide in mice after intravenous administration, *Carbon*, 2011, **49**(3), 986–995.

100 M. C. Duch, G. S. Budinger, Y. T. Liang, S. Soberanes, D. Urich, S. E. Chiarella, L. A. Campochiaro, A. Gonzalez, N. S. Chandel, M. C. Hersam and G. M. Mutlu, Minimizing oxidation and stable nanoscale dispersion improves the biocompatibility of graphene in the lung, *Nano Lett.*, 2011, **11**(12), 5201–5207.

101 J. Zhu, M. Xu, M. Gao, Z. Zhang, Y. Xu, T. Xia and S. Liu, Graphene oxide induced perturbation to plasma membrane and cytoskeletal meshwork sensitize cancer cells to chemotherapeutic agents, *ACS Nano*, 2017, **11**(3), 2637–2651.

102 M. C. P. Mendonça, E. S. Soares, M. B. de Jesus, H. J. Ceragioli, S. P. Irazusta, A. G. Batista, M. A. Vinolo, M. R. Maróstica Júnior and M. A. da Cruz-Höfling, Reduced graphene oxide, nanotoxicological profile in rats, *J. Nanobiotechnol.*, 2016, **14**(1), 53.

103 M. Xie, H. Lei, Y. Zhang, Y. Xu, S. Shen, Y. Ge, H. Li and J. Xie, Non-covalent modification of graphene oxide nano-composites with chitosan/dextran and its application in drug delivery, *RSC Adv.*, 2016, **6**(11), 9328–9337.

104 K. Yang, J. Wan, S. Zhang, Y. Zhang, S. T. Lee and Z. Liu, *In vivo* pharmacokinetics, long-term biodistribution, and toxicology of PEGylated graphene in mice, *ACS Nano*, 2010, **5**(1), 516–522.

105 N. Luo, J. K. Weber, S. Wang, B. Luan, H. Yue, X. Xi, J. Du, Z. Yang, W. Wei, R. Zhou and G. Ma, PEGylated graphene oxide elicits strong immunological responses despite surface passivation, *Nat. Commun.*, 2017, **8**, 14537.

106 S. Zhang, K. Yang, L. Feng and Z. Liu, *In vitro* and *in vivo* behaviors of dextran functionalized graphene, *Carbon*, 2011, **49**(12), 4040–4049.

107 H. H. Gustafson, D. Holt-Casper, D. W. Grainger and H. Ghandehari, Nanoparticle uptake, the phagocyte problem, *Nano Today*, 2015, **10**(4), 487–510.

108 S. P. Mukherjee, A. R. Gliga, B. Lazzaretto, B. Brandner, M. Fielden, C. Vogt, L. Newman, A. F. Rodrigues, W. Shao, P. M. Fournier, M. S. Toprak, A. Star, K. Kostarelos, K. Bhattacharya and B. Fadeel, Graphene oxide is degraded by neutrophils and the degradation products are non-genotoxic, *Nanoscale*, 2018, **10**(3), 1180–1188.

109 R. Kurapati, J. Russier, M. A. Squillaci, E. Treossi, C. Ménard-Moyon, A. E. Del Rio-Castillo, E. Vazquez, P. Samorì, V. Palermo and A. Bianco, Dispersibility-Dependent Biodegradation of Graphene Oxide by Myelo-peroxidase, *Small*, 2015, **11**(32), 3985–3994.

110 C. M. Girish, A. Sasidharan, G. S. Gowd, S. Nair and M. Koyakutty, Confocal Raman imaging study showing macrophage mediated biodegradation of graphene *in vivo*, *Adv. Healthcare Mater.*, 2013, **2**(11), 1489–1500.

111 G. Reina, J. M. González-Domínguez, A. Criado, E. Vázquez, A. Bianco and M. Prato, Promises, facts and challenges for graphene in biomedical applications, *Chem. Soc. Rev.*, 2017, **46**(15), 4400–4416.

112 L. Ou, B. Song, H. Liang, J. Liu, X. Feng, B. Deng, T. Sun and L. Shao, Toxicity of graphene-family nanoparticles, a general review of the origins and mechanisms, *Part. Fibre Toxicol.*, 2016, **13**(1), 57.

113 R. Dal Magro, B. Albertini, S. Beretta, R. Rigolio, E. Donzelli, A. Chiorazzi, M. Ricci, P. Blasi and G. Sancini, Artificial apolipoprotein corona enables nanoparticle brain targeting, *Nanomedicine*, 2018, **14**(2), 429–438.

114 Y. Wei and L. Zhao, Passive lung-targeted drug delivery systems *via* intravenous administration, *Pharm. Dev. Technol.*, 2014, **19**(2), 129–136.

115 M. Papi and G. Caracciolo, Principal component analysis of personalized biomolecular corona data for early disease detection, *Nano Today*, 2018, **21**, 14–17.

116 V. Serpooshan, M. Mahmoudi, M. Zhao, K. Wei, S. Sivanesan, K. Motamedchaboki, A. V. Malkovskiy, A. B. Gladstone, J. E. Cohen, P. C. Yang, J. Rajadas, D. Bernstein, Y. J. Woo and P. Ruiz-Lozano, Protein corona influences cell–biomaterial interactions in nanostructured tissue engineering scaffolds, *Adv. Funct. Mater.*, 2015, **25**(28), 4379–4389.